Power Electronics and Drives
Volume 5(40), 2020 DOI: 10.2478/pead-2020-0001

Power Electronics and Drives

A Review of Methods and Challenges for Improvement in Efficiency and Distance for Wireless Power Transfer Applications

Review Article

Sokol Kuka, Kai Ni*, Mohammed Alkahtani

The Department of Electrical Engineering and Electronics, University of Liverpool, 9 Brownlow Hill, Liverpool L69 3GJ, United Kingdom

Received May 06, 2019; Accepted August 23, 2019

Abstract: Over the past few years, interest and research in wireless power transfer (WPT) have been rapidly incrementing, and as an effect, this is a remarkable technology in many electronic devices, electric vehicles and medical devices. However, most of the applications have been limited to very close distances because of efficiency concerns. Even though the inductive power transfer technique is becoming relatively mature, it has not shown near-field results more than a few metres away transmission. This review is focused on two fundamental aspects: the power efficiency and the transmission distance in WPT systems. Introducing the principles and the boundaries, scientific articles will be reviewed and discussed in terms of their methods and respective challenges. This paper also shows more important results in efficiency and distance obtained, clearly explaining the theory behind and obstacles to overcome. Furthermore, an overlook in other aspects and the latest research studies for this technology will be given. Moreover, new issues have been raised including safety and security.

Keywords: *wireless power transfer • inductive power transfer technique • efficiency • distance • safety • security*

1. Introduction

The use of wireless power transfer (WPT) for many electrical equipment is seen as powerful new technology. Delivering power through a long-distance is fascinating for the future. The wireless charging is identified as a great substitute of the wirings and batteries on many electrical devices. Wirings give enough power, but restrict the mobility and have safety issues. On the other hand, batteries offer great mobility but have initial high cost and limited life (Market Research Future, 2019). For these reasons, the WPT researches are very important and a big step forward has been made in recent years. They have a great number of applications, such as in electric vehicles (EV), where the maximum mileage run is strictly tied to the battery capacity. Increasing the number of batteries in each EV will be straight reflected in their price. Also, it is necessary to consider the amount of time spent on charging and anxiety for the users to run out of power.

To overcome these problems, fast wireless charging has been applied in vehicles for public transportation in the traditional stations (Musavi and Eberle, 2014). This type of application has itself a waiting time and short distance between stations that it has been easily adopted the WPT for electrical charging. Moreover, the researches for EV wireless charging while driving or parking (Zhang and Chau, 2015; Sato et al., 2016) are very attractive and boosting the market (Markets and Markets, 2019). Another example is the diffusion of the so-called consumer electronics. Presenting the problem of a limited duration of battery life, this sector has already seen commercial achievements of these WPT systems, especially for smartphones chargers. The advantages of employing a WPT system are certainly highlighted in implantable equipment for health care (RamRakhyani and Lazzi, 2013) although it is challenging to realize such applications because the power has to penetrate a dense medium like the skin. The wireless power delivery eliminates the need for transdermal or

* *E-mail: k.ni@student.liverpool.ac.uk*

percutaneous wires, which can be cumbersome and prone to infection. Packaged batteries can only power these implants for a fixed lifetime, based on functionality and usage (Campi et al., 2016), while surgical intervention is required each time to replace them. This leads to a smaller size and lighter weight or elimination of an energy storage element that brings comfort to the patient. In all these applications, the transmission distance plays a crucial role in the efficiency and consequently incorrect functionality of the application. If the EV, the electronic device and the implant are far enough to not receive a certain level of power, they will not be charged and then will not be working. There are several ways in which energy could be transmitted, and they could be classified according to their working ranges, namely the far-field (long distance) and the near-field (short distance) transmission (Garnica et al., 2013). In the far-field range, the power is transmitted through microwaves and has been developed for low-power applications practically because of its low efficiency. The radio frequency (RF) signals have powered very low power application and it is more considered as a harvesting energy solution (Marian et al., 2012). The ultrasound waves have been utilised in similar applications (Charthad et al., 2015; Tsuji et al., 1993). They are converted through the piezoelectric effect as a transducer for the electrical signal. Although with low intensity, the light rays can transmit power. For instance, sun rays are possible to generate a large amount of energy despite travelling enormous distances. Similar to the other far-field sources, the power generation could happen certainly in particular conditions and vast size (Jarvis et al., 2013; Kimmich, 1982; Fakidis et al., 2016). Great use of this technique will be the solar farms in large areas of Saudi Arabia, which can generate up to 80 GWh of electricity per year (Almasoud and Gandayh, 2015). The near-field WPT is a better option because of the high power transmitted (Kim et al., 2018). It is physically based on the electric and magnetic fields (Dai and Ludois, 2015) created in capacitors layers, namely capacitive power transfer (CPT) and mutual inductors as inductive power transfer (IPT) (Balanis, 2005; Theodoridis, 2012) as shown in Fig. 1. The advantage of CPT is that it could be used efficiently for penetrating solid materials. However, their applications are limited because of the layer available area, the dielectric's cost and the minimum distance between the electrodes. It has mostly been applied to low power devices (Ching and Wong, 2013). On the other hand, the IPT systems are based on the magnetic field link in mutually inducted coils. The IPT systems are divided into two categories, namely loosely coupled system (LCS) and tightly coupled system (TCS). In TCSs, the coupling factor (coefficient) k is close to unity; therefore, the transferred power efficiency is quite high. A well-known application for TCS is a power transformer. In LCSs, the coupling factor is quite low; depending on the application, k can range between 0.01 and 0.5 (Low et al., 2009). The reason for the low coupling factor is the absence of high permeable magnetic path between the coupled coils compared with the coil sizes.

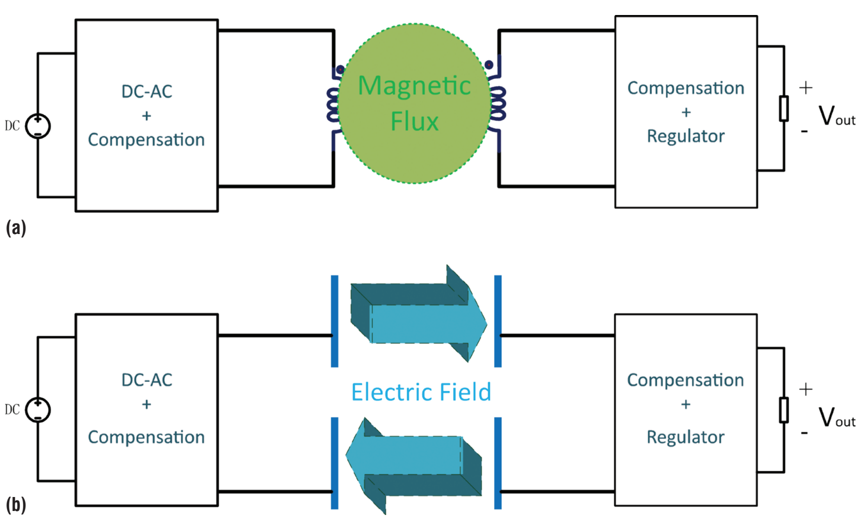

Fig. 1. (a) IPT based on the magnetic field in mutual inductors. (b) CPT built with capacitive layers and the electric field created.

In the literature review on WPT, there are many articles and reviews about innovative studies of WPT for the inductive transmission. Scientific articles are more focused on emphasising an important achievement in the

WPT constraints like efficiency, distance, misalignment, power converters, electromagnetic interference (EMI), security, etc. On the other hand, reviews in WPT are often an overview of the all system (Zhang et al., 2019), or only a particular part such as the power converters adopted (Jiang et al., 2017a). Due to the emerging market of EVs, there is also a great interest in publishing papers about wireless charging of EVs, including dynamic and stationary charging EVs (Yang et al., 2018). In particular, the static ones are mostly reviewed, with great emphasis on their core and coil structures, and switching techniques (Wei et al., 2014; Jiang et al., 2017b). In the last year, a considerable amount of studies focused on WPT applications have been published. Although recent WPT reviews are reported, there is less reference in one of the most important aspects such as the maximum distance achieved in the applications (Abou Houran et al., 2018). In a WPT system, the possibility to achieve long distances is very attractive but at the same time, it is very difficult. This is a major issue, as the distance between transmitter and receiver increases the efficiency plummet down. High efficiency is the other most desired requirement. Many articles reported achievements in efficiency, but there are no reviews about efficiency–distance links and methods for increasing distances (Barman et al., 2015). Nevertheless, efficiency and distance are the immediate and commercially interesting values of a WPT system. Latest applications are shown in Fig. 2 and listed in Table 1 where the most important parameters are displayed. The topic is a recent trend of research and very extensive, thus a review for the whole topic becomes long and exhausting for the reader (Abou Houran et al., 2018; Liu et al., 2018).

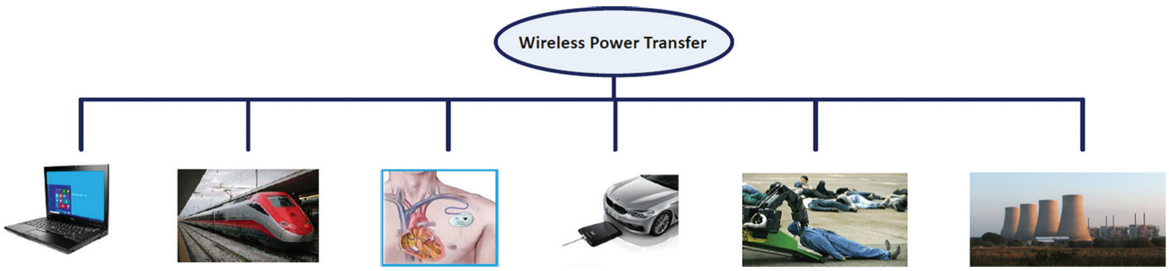

Fig. 2. Relevant applications of wireless power transfer technique.

Table 1. Interesting examples of wireless power transfer applications followed by the year, power transmitted, frequency, efficiency and distance achieved

	Lithium battery	Rail transport	Pacemaker	EV	Autonomous robot	Power plants
Year	2018 (Jawad et al., 2018)	2018 (Reatti et al., 2018)	2018 (Campi etal., 2018)	2018 (Elnail et al., 2018)	2018 (Tampubolon et al., 2018)	2018 (Choi et al., 2014a)
Power	5 W	27 kW	6.2 W	3.5 kW	1.5 kW	11.1 W
Frequency	1 MHz	25 kHz	4 MHz	85 kHz	120 kHz	20 kHz
Efficiency	53.08%	96.7%	73%	96%	80%	0.35%
Coil + Core size	30 cm	1.128 m	35 cm	50 cm	30 cm	2 m
Distance	15 cm	85 cm	30 cm	20 cm	75 cm	7 m

The purpose of this paper is to give a clear understanding about the power efficiency and distance of transmissions principles, latest research, issues and challenges to the readers. This paper categorises the latest results in efficiency and distance for WPT applications, review and discuss the issues and the challenges behind these achievements. This document is organised as follows:

- Section 2 is dedicated to efficiency. In the beginning, it will be given some basic principles of the WPT focused on some efficiency formulas. Later, the article starts considering the main components that affect efficiencies, such as the coil and the medium, the compensation network and the power converters.
- The transmission distance has been considered in Section 3 and has been classified and discussed based on the maximum range achievable: short range, medium range and long range where multi-coils systems have been analysed.
- In Section 4, a further brief review of other requirements for WPT systems is given.
- Finally, a conclusive discussion will end the paper in Section 5.

2. Principles of WPT

To begin with, a block diagram of a WPT system with the various components is shown in Fig. 3a. The system is composed of two parts: the power transmitter and the receiver. In the power transmitter section, the front-end alternating current (AC)–direct current (DC) rectifier converts the supplied AC voltage to a DC voltage to feed an inverter, which produces a high-frequency AC power output for the transmitter coil. When an AC is passing through a coil, referred to as the transmitter or primary coil, it generates an alternating magnetic field based on the Faraday's law of induction. If another coil, referred to as the receiver or secondary coil, is placed near the transmitter, then the alternating magnetic field will induce a voltage in the receiver coil and a current will flow when there is a load connected to the coil. Therefore, power is being delivered inductively from the primary coil to the secondary coil.

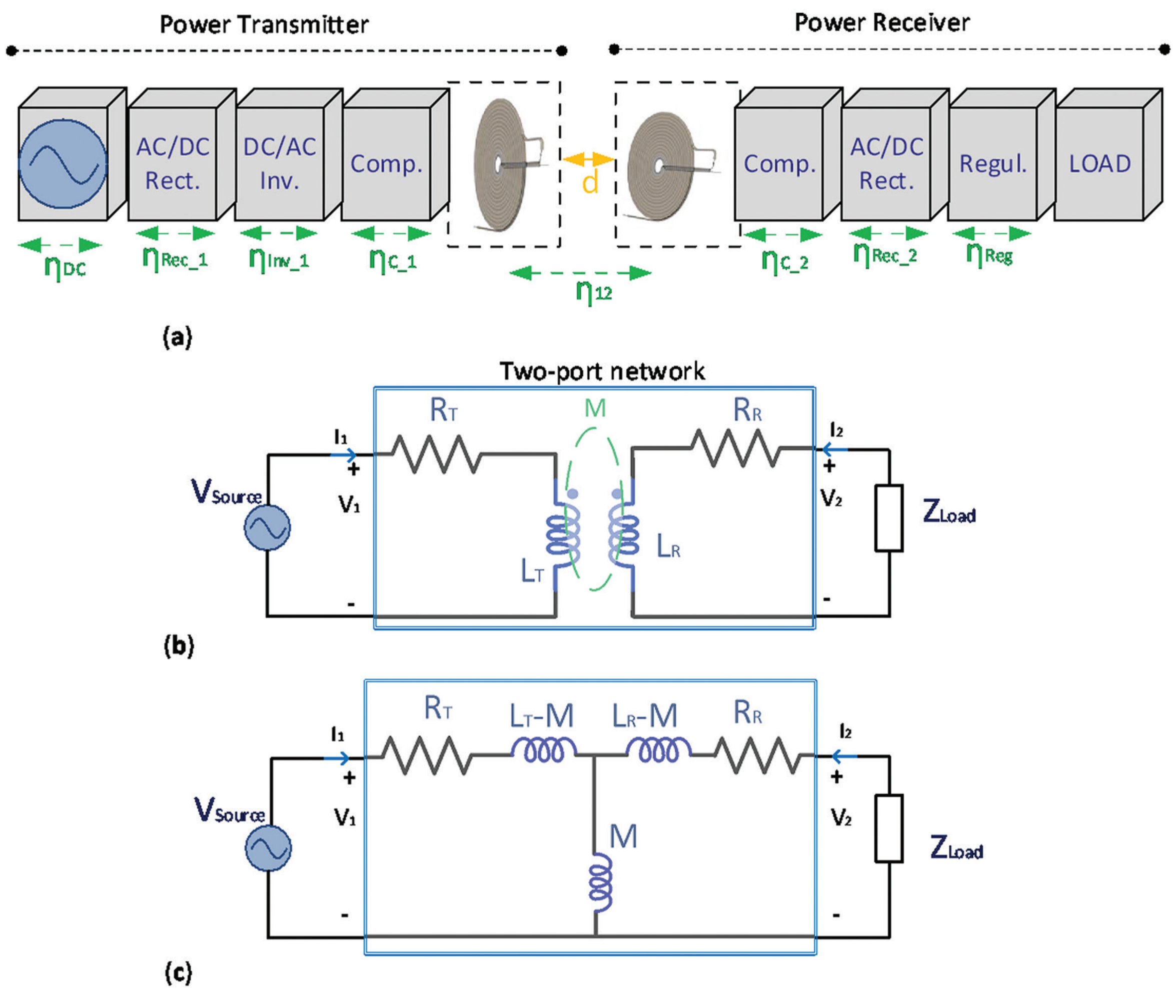

Fig. 3. (a) The block diagram of a WPT system with the various efficiencies along the transmission path considering the non-ideal source, AD/DC converter, rectifier and inverter, compensation network and coupling factor. The receiver could be symmetrical depending on the type of load. (b) Two-port network model of the coupled coils. (c) Equivalent T-model of the coupled coils.

An additional compensation or tuning network circuit is placed before the transmitting and receiving coil as a tuning block for the high-frequency AC. At this point, the high-frequency current flows through the primary coil where it is converted into a high-frequency alternating magnetic field and when it is detected by the receiving coil, it will be converted into a high-frequency alternating voltage. In the power receiver section, there is another compensation network, which tunes the operating frequency matching the transmitter. If the load to be supplied is a DC, then the AC–DC rectifier converts the AC voltage from the resonant tank to the DC voltage, ready for LEDs or rechargeable battery. Also, it is often necessary to add a regulator to keep the voltage stable when connected to a battery or load. As shown in Fig. 3a, the overall system is composed of different blocks with relative efficiency indicated in the picture. We can increase the overall η_{TOT} only by increasing the efficiency η_i of each block. In general, the efficiencies depend on the power electronic design, the topology of circuitry and their parasitic effect. Also, the magnetic link η_{12} has the critical value of the overall efficiency and it is strictly related to the distance through the k_{12} value. In additions, it also depends on outer diameter and quality factor of WPT systems. In the mutually coupled coils (often also indicated with “1“ and “2“, respectively, primary and secondary), the higher is the coupling factor k_{12} between them, the higher the efficiency η_{12} of power is delivered to the load.

Further consideration of the coils shape design, which affects the self-inductances of the coils is explained in the next subsections. To the self-inductances of each coil, a third inductance exists between the two coils, which is referred to as the mutual inductance M:

$$M = K_{12}\sqrt{L_T L_R} \tag{1}$$

where k_{12} is the coupling factor and L_T and L_R are self-inductances of the transmitter and receiver coil, respectively. A two-port equivalent analysis allows to find out significant expressions for the efficiency η_{12} in a simple way. Considering the coils connected directly to an equivalent voltage source, it will be considered the Z-parameters of the block highlighted in blue shown in Fig. 3c. The resistances R_T and R_R are wire resistances of the coils, avoiding impedances from other blocks as illustrated previously in Fig. 3b. The system is evaluated as:

$$\begin{vmatrix} V_{Source} \\ V_{Load} \end{vmatrix} = \begin{vmatrix} Z_{11} & Z_{12} \\ Z_{21} & Z_{22} \end{vmatrix} \begin{vmatrix} I_1 \\ I_2 \end{vmatrix} = \begin{vmatrix} R_T + j\omega L_T & j\omega M \\ j\omega M & R_R + j\omega L_R \end{vmatrix} \begin{vmatrix} I_1 \\ I_2 \end{vmatrix} \tag{2}$$

where the values for the Z-parameters are taken from the two-port network in Fig. 3c. The impedance seen by the power source inverter is a key parameter that directly contributes to the inverter, link, efficiencies of other blocks, along with voltage gain and maximum WPT. The input impedance Z_{in} sought by the V_{Source} using Eq. (2) can be calculated as:

$$Z_{in} = Z_{11} - \frac{Z_{12}^2}{Z_{22} + Z_{Load}} = R_T + j\omega L_T + \frac{\omega^2 M^2}{R_R + j\omega L_R + Z_{Load}} \tag{3}$$

where the first part is the transmitter impedance. The second part of this impedance is an important value and it is also known as the impedance reflected from the receiver. Indicated with $Z_{ref,T}$ this value is given by:

$$Z_{ref,\,T} = \frac{\omega^2 M^2}{Z_2 + Z_{Load}} = \frac{\omega^2 k^2 L_T L_R}{Z_2 + Z_{Load}} \tag{4}$$

where Z_2 is the impedance of the receiver, which is the value of the coil self-impedance plus additional compensation network not shown in Fig. 2c. The efficiency or the operating power gain G_P of an electric circuit is the ratio of power transferred to the load (considering the load pure resistive) from the power entering into the network. Thus, this gain is independent of the source impedance and is usually referred to as the power transmission efficiency η_{12}.

$$\eta_{12} = G_P = \frac{P_{Load}}{P_{in}} = \frac{|I_R|^2 \operatorname{Re}\{Z_{Load}\}}{|I_T|^2 \operatorname{Re}\{Z_{in}\}} = \frac{R_{Load}}{R_T \frac{L_R^2}{M^2} + (R_R + R_{Load})\left[1 + \frac{R_T(R_R + R_{Load})}{\omega^2 M^2}\right]} \tag{5}$$

When the angular frequency ω_0 at the system operating frequency f_0 is high enough, the denominator decreases and when:

$$\omega_0^2 \gg \frac{R_T\left(R_R + R_{Load}\right)}{M^2} \tag{6}$$

the efficiency is at its maximum value where η_{12max} results:

$$\eta_{12max} = \frac{R_{Load}}{R_T \frac{L_R^2}{M^2} + \left(R_R + R_{Load}\right)} \tag{7}$$

Equation (6) introduces the importance of adopting a relatively high operating frequency at the power capability and is the most important specification for WPT applications (Kazmierkowski and Moradewicz, 2012; Sample et al., 2011). On the other hand, at the higher operating frequency, the power level is limited by the topology of power converters, parasitic, switching devices and related control mechanism. As seen in Eq. (4), the system depends on the type of the load Z_{Load} which in optimal conditions (maximum efficiency) could be found in a derivation of Eq. (7) as:

$$\frac{\delta \eta_{12}}{\delta R_{Load}} = 0 \rightarrow Z_{Load,OPT} = R_R \sqrt{1 + k_{12}^2 Q_T Q_R} - j\omega L_R \tag{8}$$

where $Q_T = \frac{\omega L_T}{R_T}$ and $Q_R = \frac{\omega L_R}{R_R}$ represent the quality factors of the transmitter and receiver coils, respectively. To achieve the peak of efficiency [Eq. (8)] and have no reactive power on the load [zero phase angle (ZPA)], an impedance matching is required. In the compensation network, there is a capacitive impedance (a capacitor or a more complex circuit) to cancel the reactance ωL_R. More alternatives will be given in Section 3.2. The formed LC resonant tank will give a pure resistive optimum load:

$$R_{Load,\ OPT} = R_R \sqrt{1 + k_{12}^2 Q_T Q_R} \tag{9}$$

By substituting the resistive optimum load back into Eq. (5) and expressed in function of the coupling factor and quality factors, the maximum power transmission efficiency is given by:

$$\eta_{12max} = \frac{k_{12}^2 Q_T Q_R}{\left(1 + \sqrt{1 + k_{12}^2 Q_T Q_R}\right)^2} = \frac{\Delta}{\left(1 + \sqrt{1 + \Delta}\right)^2} \tag{10}$$

where $\Delta = k_{12}^2 Q_T Q_R$, which is also called the figure of merit (FoM) of the system where maximum efficiency can be at least 17% when Δ is large than 1 (Kurs et al., 2007). And this condition is referred to as the *strongly coupled resonance regime* that is completely different from the coupling factor *k*. This is a method used in WPT applications where it is desired long distance in front of an acceptable power delivered. The WPT system is still loosely coupled but can operate in strongly coupled magnetic resonance regime, only if the quality factors Q_T and Q_R are designed to be enough high. Increasing Q_T and Q_R will keep a relatively good efficiency. Quality factors that can reach the value of 1000 or even higher. This value could be achieved by choosing designing coils with lower inner resistance (Onar et al., 2013) or a high-operating frequency and this method is introduced in Sections 4.1 and 4.2.

3. Distance in WPT Systems

The near-field transmission is also divided into two parts according to the wavelength λ; the reactive (non-radiative, mostly inductive) region and the radiative region (Umenei, 2019). The boundary between regions is commonly defined as the distance from the source to 0.159 λ. In this way for operating frequency f_0 from 10 kHz to 1 GHz, it is possible to calculate the maximum physical distance reachable, which are boundaries of the reactive and radiative near-field regions. These values are listed in Table 2.

Table 2. Theoretical maximum distance reachable by the WPT in the reactive and radiative region (Lee and Cho, 2013)

Range–frequency	1 GHz	100 MHz	10 MHz	1 MHz	100 kHz	10 kHz
Reactive region (m)	0 − 0.05	0 − 0.48	0 − 4.77	0 − 47.7	0 − 477.5	0 − 4775
Radiative region (m)	0.05 − 0.3	0.48 − 3	4.77 − 30	46.6 − 300	477.5 − 3000	4775 − 30,000

The reactive near field can be further classified into the short range and the middle range. The short range is realized when the distance between the coils is smaller than the size of the primary coil. Whereas, the middle range happens when the distance is at least 2–3 of the geometry of the devices (Kurs et al., 2007). This is not a strict definition, but the middle range distance is at least larger than the size (length or diameter) of the transmitter coil (Hui et al., 2014). For distances $d \gg r_T$ and $d \gg r_R$, the relationship among coupling factor, size and distance is shown in the following equation:

$$k_{12} \approx \frac{1}{2\left(\frac{d}{\sqrt{r_T r_R}}\right)^3} \tag{11}$$

where d is the distance between coils; r_T and r_R are the transmitter and receiver coil radius, respectively (Mur-Miranda et al., 2010). The transmission distances for these systems are all within a fraction of the geometry of the transmitter coil or pad. The reason is that the coupling coefficient between the coils decays as $1/d^3$ from the source coil in the near field. High efficiency is achieved when the distance is around the dimension of the coil. However, the system energy efficiency still falls rapidly when the transmission distance exceeds the dimension of the transmitter coil. Nonetheless, high efficiency can still be achieved by designing high-quality factor transmitter and receiver coils and by using a soft-switching power converter to lower the impedance of the power source. For instance with this method, using a transmitter (with radius r_T = 15 cm and quality factor Q_T = 1270) and a receiver (with radius r_T = 10 cm and quality factor Q_R = 1100), the system can transfer 105 W to the load over a distance of 30 cm with a system efficiency of 77% (Hui et al., 2014). If the distance far exceeds the size of the coils, the efficiency of the system will decrease rapidly because the coupling factor k becomes too small. In Mur-Miranda et al. (2010), a pair of identical resonators with a quality factor of 1000 can transfer energy through a distance of nine times its radius, but the efficiency is reduced to 10%.

3.1 Short and medium range

The power transfer in short transmission distance is commonly achievable with good coupling factor, which depends on the medium between coils whether it is air or any material with permeability one or above. Also, the best coupling factor is obtained when the coils have the same dimensions, negligible gap and they are perfectly aligned. The alignment of the transmitter not correct with the receiver has been the first challenge to overcome in this technology. Therefore, the charging appliance is usually fabricated in a similar size to have a visible matching. Although the system efficiency and power transferred can be maximized, the following problems can arise in these systems:

- Cross-talking or localized charging happens if the transmitter is much larger than the receiver. The magnetic flux path should only occur between the transmitter coil and the receiver coil. Only the transmitter coil that is closest to the receiver is powered on with others around in standby mode. This type of WPT is mostly used on dynamic EV charging applications where power consumption by each transmitter coil can be monitored to roughly identify the position of the receiving coil.

- The not alignment between primary–secondary coil is usually measured in degrees, from perfectly aligned 0° up to the coils orthogonally each other. Beyond the same size mentioned previously, another solution could be adopting a movable transmitter coil to align it at the position of the receiving coil, which is detected through certain sensors was once proposed by the Qi standard. The transmitter coil will be moved to the place right beneath the receiving coil. This solution has a great potential in the stationary EV charging because precisely adjusting the position of the vehicle is relatively difficult especially when the receiving coil is very small. A further solution is to make sure that the receiver coil position is constrained by the magnetic attraction or the incorporated mechanical guide.

Particular note should be taken for the misalignment in biomedical implants where the receiver has dimensions of millimetres, often not anchored and completely hidden inside the patient body. Moreover, the medium is not air but human issue: by taking into account the higher absorption rate, in Mirbozorgi et al. (2017) an optimal design scheme was proposed by using a large external transmitting coil, which can effectively energize the implant in the brain tissue. In the radiative near-field region for the millimetre-scale receiver, there are research applications as a cardiac implant (Galbraith et al., 1987; Ho et al., 2013). Relative high efficiencies can be obtained when the system operates in the low gigahertz range, which is suitable for the biomedical implantable system.

For medium-range applications, there is a vast amount of studies. Most of the literature is focused on the electric vehicle (EV) wireless charging. Recent articles and reviews on EV can be classified about their focus:

- Coil design, operating frequency and misalignment (Patil et al., 2018).
- Static versus dynamic charging and consideration on energy grid management (Ahmad et al., 2018).
- Power density, challenges and market trades off (Bosshard and Kolar, 2016).

3.2 Long range: multi-coil design

Multiple coils in the transmitter, receiver, or in the middle are adopted essentially for two main reasons: (a) more degrees of freedom to maximize the efficiency and desensitize the link gain versus coupling factor and (b) highly coupled transmitter-repeater or repeater-receiver link work greatly as impedance matching elements at both sides. Although this last configuration requires four or more coils, it offers a better efficiency–distance than a three coils system. For this reason, the three coil WPT is not very popular, unless the application has no space for additional coils.

Let us consider a four-coil resonator system with two intermediate repeaters coils called “2“ and “3“ where an impedance (capacitor) compensation Z_2 and Z_3 are connected to form LC resonators. As shown in Fig. 4, the transmitter and receiver are referred to as “1“ and “4“, respectively. It has been considered the transmitter R_T and the load impedance Z_{Load} having a relatively low-quality factor of $Q_T = Q_1$ and $Q_R = Q_4$. Considering only the parasitic resistance, much higher quality factor Q_2 and Q_3 can be achieved. With this new nomination, k_{23} will be much lower than k_{12} and k_{34} because the distance between the intermediate coils is usually larger than the dimensions of the coils. In this way, the cross-coupling effect could be neglected because of either the low-quality factor Q or the small coupling factor depicted in Fig. 4 in yellowish-green. Similar to the two-coil system, the FoM could be written as a generic Δ_{ij} for any two of the four coils:

$$\Delta_{ij} = k_{ij}^2 Q_i Q_j \tag{12}$$

calling *i* and *j* the number of the referred coils. An important equation to notice in the design of a multi-coils system comes from the impedance reflected from all coils to the primary transmitter. Considering Eq. (4) introduced in a two-coil system, it is possible to write for each coil the reflected impedance:

$$\begin{cases} Z_{ref,\,3} = \dfrac{\omega^2 k_{34}^2 L_3 L_4}{Z_4 + Z_{Load}} \\ Z_{ref,\,2} = \dfrac{\omega^2 k_{23}^2 L_2 L_3}{Z_3} \\ Z_{ref,\,1} = \dfrac{\omega^2 k_{12}^2 L_1 L_2}{Z_2} \end{cases} \tag{13}$$

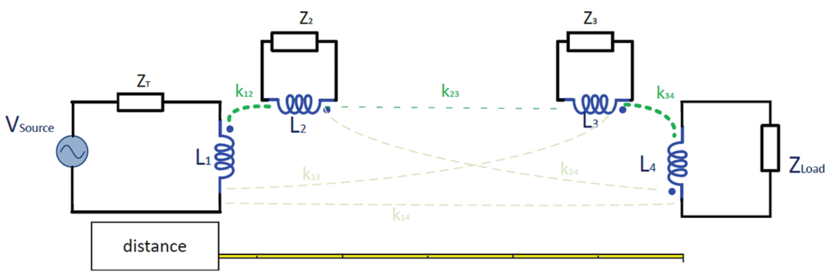

Fig. 4. Four coils WPT system with the coupling factors. The couplings are marked following their value. k_{13}, k_{14} and k_{24} are not visible because their intensity values are negligible.

Combining these equations in the 13 last equation, it is possible to obtain the impedance reflected in the primary transmitter:

$$Z_{ref,\ 1} = \cfrac{\omega^2 k_{12}^2 L_1 L_2}{\cfrac{\omega^2 k_{23}^2 L_2 L_3}{\cfrac{\omega^2 k_{34}^2 L_3 L_4}{Z_4 + Z_{Load}} + Z_3} + Z_2} \tag{14}$$

when simplifying we obtain:

$$Z_{ref,\ 1} = \frac{\omega^2 \left(\frac{k_{12} k_{34}}{k_{23}}\right)^2 L_1 L_4}{Z_4 + Z_{Load}} = \frac{\omega^2 k_{TOT}^2 L_1 L_4}{Z_4 + Z_{Load}} \tag{15}$$

In this equation, we can notice that the reflected impedance of all system depends directly only by the total coupling factor and the value of receiver impedance. Moreover, the WPT system can be seen as an equivalent total coupling factor defined by:

$$k_{TOT} = \frac{k_{12} k_{34}}{k_{23}} \tag{16}$$

It is a design rule making sure that the following condition can be met:

$$k_{TOT} = \frac{k_{12} k_{34}}{k_{23}} = 1 \tag{17}$$

the reflected load will be matched and we will have the maximum power transferred. In such a way, the four coils system creates a possibility to extend the distance from primary to the load using more and more coils. The transmission distance can be elongated keeping high total coupling factors even if the mutual coupling factor between the repeaters is very low. Additional intermediate coils with loose coupling between them are adopted in order to increase the total coupling factor between the transmitter and the receiver. In this method, the low coupling is advantageous. For example, even if the coefficient k_{23} between the intermediate coils is loosely coupled to 0.01 because of the long transmission distance, the equivalent coupling coefficient k_{TOT} of the whole system can still be adjusted to 1 when both k_{12} and k_{34} are considered strongly coupled set to 0.1.

However, the impedance matching such a system is not endowed with high overall efficiency because it is restricted by the merit factor given by Eq. (19). Nonetheless, the four-coil system still offers (in terms of efficiency–distance) a better solution rather than the two-coil systems when the distance is much bigger than the coil size. A similar system is reported by the Massachusetts Institute of Technology (MIT) research group which could deliver 60 W power over a distance of 2 m long (Kurs et al., 2007). The distance achieved is more than four times of the transmitter coil size (30 cm), albeit the efficiency 15% between the intermediate coils.

The major issue for the multi-coils system comes from the frequency splitting phenomenon, which has been studied in Sample et al. (2011). The reason is the relationship between coupling factor and distance considered in Eqs (4) and (18) for the impedance reflected. In other words, the mutual coupling factor k is inversely proportional to the distance d, therefore increasing d means decreasing k. To avoid the complication of frequency splitting, few adaptive matching methods based on frequency tracking have been introduced (Park et al., 2011; Hoang and Bien, 2012). Furthermore, it has been illustrated in Lee et al. (2015) that antiparallel resonance loops are adopted to cancel the effects of frequency splitting. Other researches have covered new areas, such as multiple transmitters (Ahn and Hong, 2013; Yoon and Ling, 2011) and multiple receivers (Cannon et al., 2009; Kim et al., 2010). However, because of the limitation of energy efficiency, it has been used only for low power WPT systems.

4. Latest Research Studies

The latest research studies can be classified into five groups as shown in Fig. 5. The most important factor in the WPT system is the coil geometry (structure), which helps to increase the distance and efficiency in any applications. As introduced in Eq. (10), one method is to increase the quality factors of the coils to improve the efficiency although low coupling factor. Later through the choice of compensation network, we can achieve maximum power transfer to the load as shown in Eq. (8). Also, there are some well-known methods of power conversion that improve efficiency.

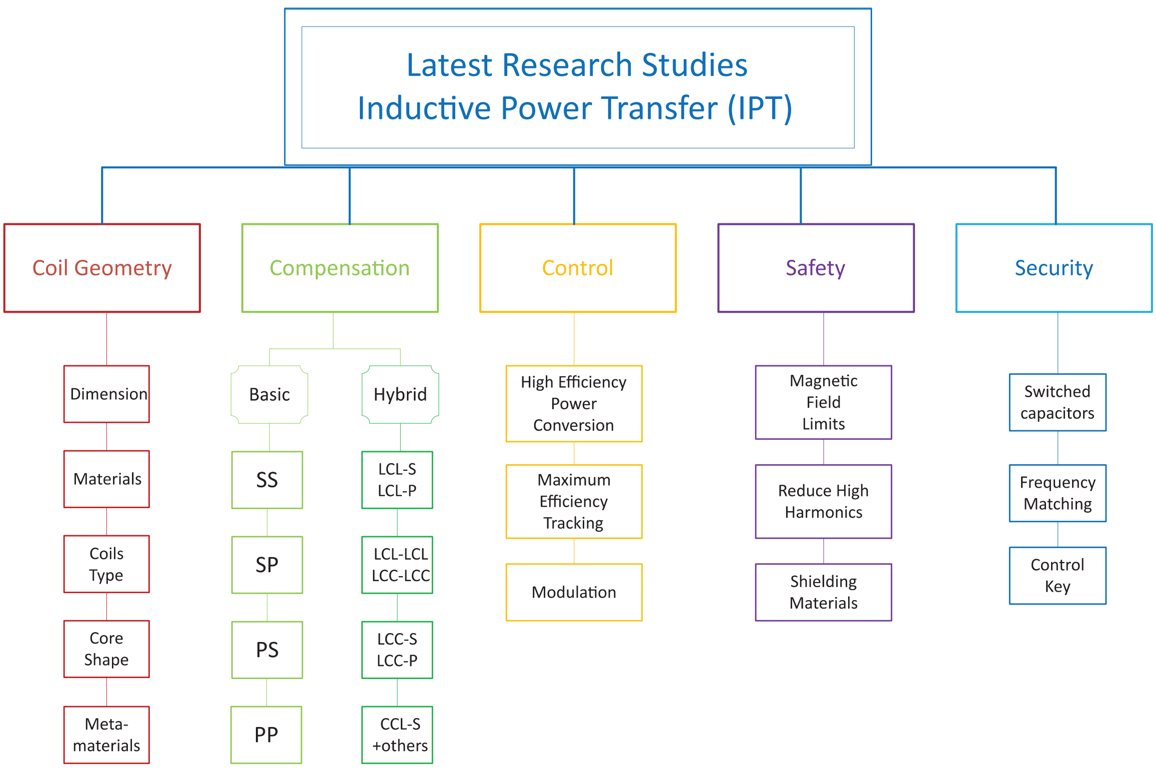

Fig. 5. Classification of the improvements in the latest research studies in IPT.

4.1 Coil geometry and core

The coil design is an initial step in WPT system since it determines the value of self-inductance, which depends on the size, length, geometry, cross-sectional area, the separation between turns, number of turns and thickness or width of copper. The formula for several coils shape, like circular, square, rectangle, etc., is given in Thompson (1991) and Grover (2004). For on-chip design, the layout depends on different factors that are given in Mohan (1999). These formulas could be very complex. The most used on-chip coil shape is spiral (Pancake spiral coil), and the formula is given in Khan et al. (2017) as:

$$L = \frac{N^2 r^2}{8\,r + 11\,D_i} \tag{18}$$

where

$$r = \frac{D_i + N\left(W + S\right)}{2} \tag{19}$$

In Eq. (19), L is the value of the inductance in μH, N the number of turns, r is the average winding radius in inches which is calculated by the inner diameter wire D_i, diameter W and turn spacing S (all lengths measured in inches). There is a huge amount of articles published with different solution to improve the magnetic link. In general, the design of the magnetic link includes the study of many factors, such as the coil design, distance and the type of material and conductor used in them. In many occasions, the dimension and the shape of the coil are determined by the application itself. It is important to have classified in coils categories in:

- 2D planar coils that could have a shape of a circle (Sample et al., 2011; Zhang et al., 2017), square (Lu et al., 2016; Moon and Moon, 2016), rectangle (Ahn and Hong, 2014; Li et al., 2014), planar printed spiral coils (PSC) (Chen and Zhao, 2013; Jolani et al., 2014) pancake coils (Yi et al., 2015), octagon (Park et al., 2016) and a double D shape (DD) (Zhang et al., 2015a) for EV charging. Furthermore, the WPT system in the printed circuit board (PCB) (Mohan, 1999; Song et al., 2014; Kim et al., 2015b).
- 3D coils conical loop (Yang and Tsunekawa, 2014; Zhang et al., 2015c) and helix coils (Hadadtehrani et al., 2016) mostly for charging human implanted devices, bowl-shaped transmitter coils (Campi et al., 2016), cylindrical coils (Zhang et al., 2012) simply printed on the internal or plastic external ID cover.
- Ferrites materials in which core of the coils are made of. These are non-conventional materials in WPT application. For instance, aluminium is used in Song et al. (2014), or superconductors to increase the quality factor of the coils in Jeong et al. (2016).
- Cores that increase coupling factor with an E-shape and U-shape (Li et al., 2015a; Shin et al., 2014) or a dipole (Tampubolon et al., 2018) delivering power up to a 7-m distance. Furthermore, in transportation tracks are used as core (Kim et al., 2015a; Ko and Jang, 2013).

In previous studies, there are several attempts for varying distance to be solved. In this way, the compensation network built with a capacitor matrix could deal with the frequency mismatch caused by the varying transmission distance (Lim et al., 2014). To increase the efficiency of a WPT system modelling the density of the uniform magnetic flux, Chabalko and Sample (2014, 2015) fed the natural electromagnetic transmission energy of a metal form of the cave to different receivers placed in the air space. The results in Chabalko and Sample (2015) show that a 3.96-m test cavity can feed a receiver with a radius of 3.81 cm. The energy efficiency has increased by more than 50%. The authors of Chabalko and Sample (2015) and Mei et al. (2017) also study 3D WPT systems based on the hollow mode. A 3D WPT system has been proposed for biomedical implants by Mei et al. (2017), which develops a two-axis miniaturised coil in the receiver to reduce orientation sensitivity. When energy is delivered to a mouse that runs inside the cavity cage, 93.53% of efficiency is achieved. To realise a magnetic field in all directions, Jonah et al. (2013) used orthogonal coils in the three-axis to create an orientation insensitive receiver. The measurements and the analysis indicate energy efficiency over 60% inaccurate orientation of the receiver. Choi et al. (2016) used a crossed dipole coil in an orthogonal phase to achieve 3D WPT. In this way, the insensitivity of the orientation is obtained and thanks to the 3D magnetic flux density produced.

Other methods are based on the correct choice of the medium whether it is possible. The magnetic core can be used to shape the flux path, increase the inductance, enhance the coupling and furthermore increment the distance. Although air is medium “par excellence” in WPT systems, it is important to discuss the medium because more applications are trying to adopt other solutions such as high permeability cores. Similarly to the current, the magnetic flux lines prefer the path of minimum reluctance or high permeability (the opposite of reluctance is permeability). Therefore, to increase the coupling and order the field the preferred medium to use would be a high permeable ferrite core (low reluctance). The most common ferrite materials adopted for are MnZn and NiZn (in the top part of Table 3). The first one has high permeability and high saturation flux density, while the NiZn ferrite has lower permeability and high bulk resistivity. The ferrite with high bulk resistivity reduces the induced eddy and displacement currents at higher frequencies enhancing not only the coupling factor and inductance but also the power dissipation. This makes the NiZn suitable to be used for frequencies above the megahertz (MHz). Table 3 also shows a comparison of common materials that could be used in future WPT system.

Table 3. Relative permeability list of many materials. Some of them are peak values which are obtained for a specific value of the magnetic field H and frequency indicated in the other columns. The value of the μ_R is a curve depending on the value of H. In bold the most common materials. For redundancy, values without explicit citation come from Cullity and Graham (2008)

Medium of transmission	Relative permeability“μ_R	Magnetic Field	Frequency
Electrical steel	4000 (C.R Nave Georgia State University, 2001)	0.002 T	
Ferrite–MnZn	*640*		100 kHz–1 MHz
Ferrite–NiZn	*16–640*		100 kHz–1 MHz
Carbon steel	100 (Relative Permeability Hyperphysics, 2008)	0.002 T	
Air	*1.00000037* (Cullity and Graham, 2008)		
Concrete (dry)	1		
Copper	0.999994		
Water	0.999992		
Superconductors	0		

A decisive choice is also the layout of the coil. Reducing the coil winding resistance is an important step as it improves the quality factor and link efficiency thus the maximum distance achievable. Depending on the operating frequency, the winding conductor can be solid, foil, tubular or Litz. Solid wire is a building block of many types of wires, such as Litz, and understanding its behaviour is a critical step in the winding design. The power loss inside is due to the high-frequency eddy currents induced in it by the time-varying internal (skin effect) and external (proximity effect) magnetic field (Lee and Lorenz, 2013). At high frequencies mostly above a megahertz, the solid conductor (foil wire) can be superior to other conduct or types due to its low power loss, low cost and ease of manufacturing (Sullivan, 2013). The other advantages of using a foil conductor include high current-carrying capability due to large cross-sectional area and improved thermal performance. In this way, the inductors with low overall thickness can be designed. Copper foils with thickness close to skin depth in the multi megahertz frequency range (Cu skin depth is between 65 and 15 μm in the 1–20 MHz) are commercially available and affordable. Another way to reduce the AC resistance is the Litz wire (twisting strands): the conductor needs to be divided into multiple insulated skin depth sized strands, with each strand seeing the same amount of magnetic flux (Etemadrezaei and Lukic, 2016). This is a common choice of inductor wire at frequencies up to few megahertz, above which the need for very thin strands (close to skin depth) makes the manufacturing expensive. The complete structures of the coil, including the number of turns, layers, distance between them and existence of ferrite core, are the design parameters for minimising proximity effect and AC resistance.

Recently, an artificial material has been built by the scientific community with *negative permeability* and *negative permittivity* (Alphones and Sampath, 2015). This metamaterial named as left-handed material (Bilotti and Sevgi, 2012; Kim, 2009) possesses abilities to amplify the evanescent flux lines and concentrating the electromagnetic field. Therefore, the metamaterials exhibit greater potentials to enhance the efficiency and distance in WPT systems. Wang and Teo (2012) created WPT prototypes with various metamaterial topologies for comparison and they achieved to light a 40 W bulb with distant 50 cm at 27.12 MHz. Later on, Ranaweera et al. (2014) proposed a 3D left-handed structure that has been for midrange WPT applications at 6.5 MHz, using also three turns spiral coils with negative permeability. This experiment shows that the power delivered can be improved by 33 and 7.3% in distances such as 1.0 and 1.5 m, respectively. Moreover, this paper matches the purpose of our paper where efficiency and distance improvements for WPT systems using 3D metamaterial topology, although the metamaterial is still a research topic and is not largely available. In a distance of 1.5 m, prototypes worked with double 3D metamaterial plates in proximity of the transmitter and receiver, precisely in the front (Choi and Seo, 2010) and back (Wu et al., 2013) of the coils showing an efficiency improvement up to 80%.

4.2 Compensation network

As shown previously, an important part of the design is the choice of the resonance frequency and the network topology adopted. The chosen frequency needs to be the same in both transmitter and receiver. It is also desirable that the current and voltage of the power source are in-phase, minimising the VA rating of the power supply. The easiest way is to make sure that the relationship for operating frequency f_0 is:

$$f_0 = \frac{1}{2\pi\sqrt{L_T C_T}} = \frac{1}{2\pi\sqrt{L_R C_R}} \tag{20}$$

where the capacitors C_T and C_R are additional components that are usually added on both sides to resonate at the same operating frequency and the inductors with low overall thickness can be designed. This condition is referred to as tuned primary–secondary or transmitter–receiver. This is done by a compensation network depicted in Fig. 3a, which creates the resonance. The mismatching of the operating frequency due to parasitic leads to a slight reduction of the efficiency in the compensation network blocks and indicated for power transmitter and receiver as η_{C1} and η_{C2}, respectively. Depending on the type of the application, there are four basic compensation topologies without considering resonant circuits (Chen et al., 2013) intermediate coils (Pinuela et al., 2013) or other additional capacitance and resistance (Wang et al., 2015). These are the four basic topologies shown in Fig. 6, called the series–series (S–S), series–parallel (S–P), parallel–series (P–S) and parallel–parallel (P–P) type of circuits. In general, the secondary coil is chosen to resonate at in parallel or series. The parallel-type secondary has a voltage output type and is suitable for large loads. Furthermore, in this type, the coil parasitic capacitance can be included in the compensating capacitor in parallel. Nevertheless, the disadvantage is that resonant frequency depends on the value of load (for simplicity let consider the load resistive). The series-type secondary, on the other hand, has a current output type and is suitable for small values of resistive load. The choice of secondary compensation is mostly limited to the load requirements. The primary coil could have multiple configurations depending on the number of elements. The additional elements (capacitors and inductances) will be connected with the transmitting coil L_T. The primary series needs a higher current and lower output voltage from the switched Metal–Oxide–Semiconductor Field-Effect Transistors (MOSFETs). In contrast, the primary parallel demands a higher voltage and a lower output current. In both cases, the higher values of current increase the MOSFET driver losses, and higher voltages increase the MOSFET capacitive losses. Because none of the basic four topologies can provide ZPA for constant current (CC) or constant voltage (CV) in WTP applications, advanced topologies have been proposed (Nguyen et al., 2017; Li et al., 2014) in the resonance–compensation network between the converter and the transmitting coil (Qu et al., 2017; Feng et al., 2016). In these hybrid topologies, an extra reactance is added to the circuit, which helps for a lower switching loss compared with the S or P topologies. However, the basic four topologies are still preferred for low-voltage WPT applications. Similarly to the transmitting side, the receiving side

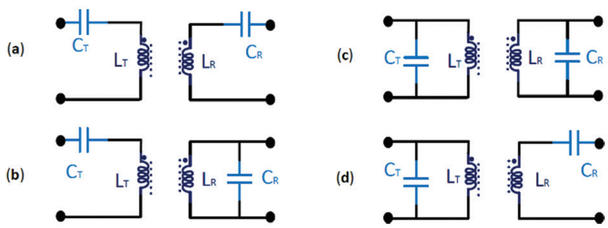

Fig. 6. The four basic topology for resonance and compensation network, namely (a) S–S, (b) S–P, (c) P–P and (d) P–S.

could have several variations, which are referred to in capital letters such as primary–secondary topology. The configuration of circuities for WPT transfer is reviewed in a few recent papers (Jiang et al., 2017a; Abou Houran et al., 2018). The LCL hybrid configuration has shown in many articles to be the most used valid alternative to the basic topologies, and a very interesting correlation has been studied in Liu et al. (2016) where S-S and S-P are compared with the LCL-S, LCL-P, LCL–LCL and S-LCL, respectively in Fig. 7a–d. In voltage source inverters, which are widely employed in WPT system, the S-S, LCL-P and LCL–LCL topologies have shown a CC in output, whereas the S-P, S-LCL and LCL-S topologies have shown a constant output voltage. For these considerations, the ones with CC to the load such as the S-S, LCL-P and LCL–LCL topologies are good candidates for battery charging applications.

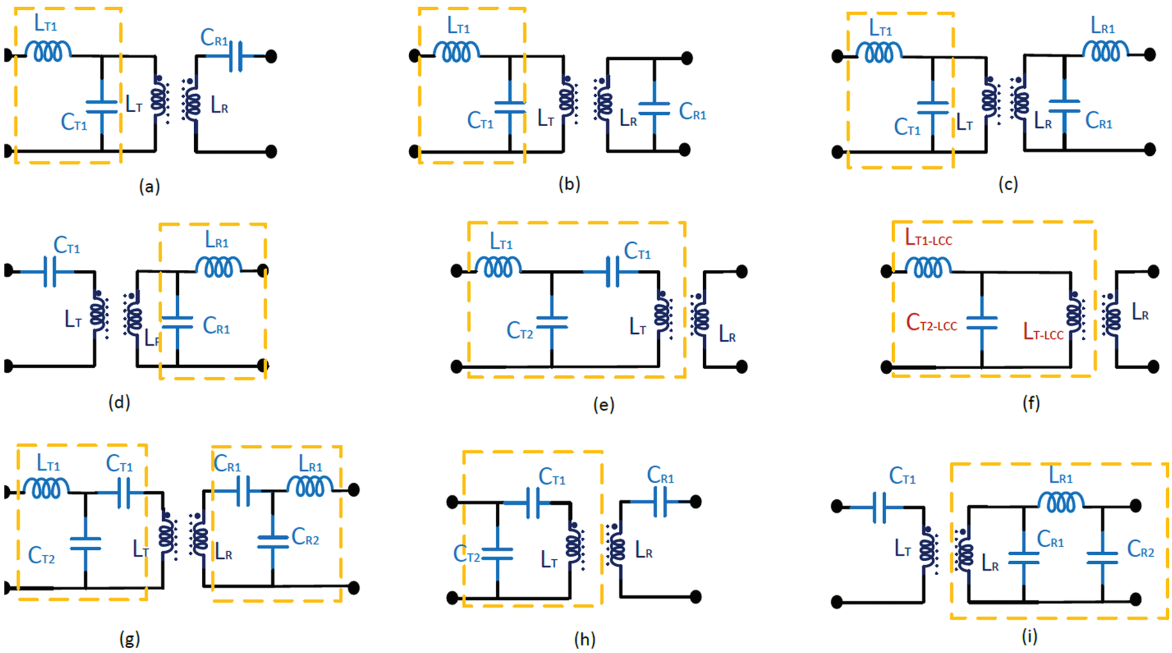

Fig. 7. Hybrid resonant topologies highlighted: the LCL configuration (L is the inductor and C the capacitor added) with the receiver in (a) series, LCL-S (b) parallel, LCL-P (c) doubled and (d) at the receiver S-LCL; (e) The LCC configuration and (f) the equivalence with LCL when voltage is driven (Li et al., 2015a). Other relevant topologies such as (g) LCC–LCC, (h) CCL-S and (i) S-CLC.

On the other hand, the S-P, S-LCL and LCL-S topologies are suitable for the electric appliances supplied by the power source of CVs. Also, the LCC topology proposed in Li et al. (2015a) can be simplified as an equivalent circuit similar to LCL topology when are driven by a sinusoidal voltage at the same operating frequency. As shown in Fig. 7f, the value of $L_{T\text{-}LCC}$, $L_{T1\text{-}LCC}$ and $C_{T2\text{-}LCC}$ could be written in function to L_T, L_{T1}, C_{T2} and C_{T1} in Fig. 7e. Therefore, the load characteristic of S-LCC, LCC-S, LCC-P and LCC-LCC (Fig. 7g) is the same as that of S-LCL, LCL-S, LCL-P and LCL-LCL, respectively, under steady-state at the same resonant frequency (Liu et al., 2016). A CCL-S hybrid topology introduced by Samanta and Rathore (2015), shown in Fig. 7h, reduces the inverter switch stress to the half of the conventional LC parallel resonant tank. Moreover, many other papers (Park et al., 2016; Lu et al., 2016) compare the characteristics of the double-sided LCC compensation topologies as considered the most suitable technology for electric vehicle (EV) wireless chargers. Wang et al. (2017) introduced the complementary S-CLC topology, in Fig. 7i, which in comparison with LCC–LCC needs fewer compensation components, meaning lower cost, smaller dimension and further greater potential in WPT applications.

Innovative compensation network for impedance matching has been shown in Chen et al. (2013). For a better performance in the distance and efficiency, Chen et al. (2013) presented a series–shunt mixed-resonant coupling in which parameters can be easily optimised for high transfer efficiency under different distances. To get the maximum power transfer, it has been analysed an LCL compensation network and inverter by Wang et al. (2004). The system was controlled by a variable frequency to find the optimal value of the inductances. In Villa et al.

(2012), a WPT for electric public transport applications, Villa et al. (2012) proposed a series–parallel–series (SPS) topology showing good results in misalignment for both the load and the transmitter. Using various frequencies, Zhang et al. (2014a) provide the maximum efficiency adopting serial and parallel compensation techniques to any load. To obtain the maximum output power, a hybrid impedance tuning scheme was developed by combining the continuous and discontinuous conduction mode (CCM–DCM), which can effectively extend the adjusting range by Seo et al. (2016).

4.3 Power converters in WPT

An advantage of inductive WPT is in applications with small size and medium- to high-power requirements. As the magnetic link size reduces, the reflected resistance to the transmitter coil gets reduced as well. To compensate for this reduction, the operating frequency needs to increase to keep the power level up. For example, in electronic devices such as phones, wearable and laptops, the power rating can range from 1 W up to about a few hundred watts. For inductive WPT in the megahertz frequency region, the operating frequency is typically bound to industrial, scientific and medical (ISM) band of 6.78 MHz, 13.56 MHz, etc. The power converter design in the megahertz region is critical as the dynamic losses increase in the switches. There are several types typically used DC–AC power inverters such as classes A, B, AB, C, D (precisely DE) and E adopted in the megahertz frequency range. The most used inverters in the WPT power applications are on switched-mode class-D and class-E power inverters as they deliver the highest efficiencies.

Due to easy system parameter design, most of the WPT applications adopt Class D full- and half-bridge inverters (Huh et al., 2011), shown in Fig. 8. The Class D inverter employs two switches and a series–resonant LC tank, which results in lower switching frequency than the Class E inverter. This topology can output twice the DC supply voltage to feed the LC resonant circuit, especially suitable for low DC supply WPT applications. The Class D resonant inverter with two switches has lower voltage stress across the switch since the peak voltage is as high as the DC supply. One of the challenges of Class D inverter in the megahertz frequency range is the switch output capacitive losses during S2 turn-on. In recent papers, the half-bridge resonant inverter has been applied to the WPT system with frequency up to 13.56 MHz (Miller et al., 2015; Wang et al., 2005). The series (S) transmitter coil requires a high amount of current that increases switch gate driver losses. On the other hand, the parallel (P) reduces the current rating of the switches by circulating it through the resonant tank. However, it produces high voltages across the switches that increase the FET output capacitive losses. A combination of SP transmitter coil would take advantage of the low voltage rating of S and low current rating of P coils. Class E inverter satisfies these conditions with doubled-tuned output circuit (Wu et al., 2012b). In Fig. 9a, the basic schematic of a class-E inverter is shown. The inverter operates between the series resonance and the one in parallel with the C_S. The capacitor C_S is referred to as the shunt capacitor and it is also an important element to achieve the zero voltage switching (ZVS) and zero-derivative switching (ZDS) conditions. Inductance L_F is referred to as the DC-feed inductance. If this inductance is large enough, the input current I_{LF} is approximately constant, which is equal to its DC component. Generally, the shunt capacitance C_S is realised by the sum of the external capacitance C_{EXT} and the MOSFET drain-to-source parasitic capacitance C_{DS}, but this value is not usually controllable. Additionally, C_S decreases as the frequency increases. Therefore, C_{DS} is dominant to C_S at high frequencies. When V_G is high, on the top of Fig. 9b then the switch is ON, the voltage across the switch V_{DS} (bottom of Fig. 9b) is approximately zero (ZVS) and the current flows through the MOSFET. During the switch OFF interval, differences of currents through the DC-feed inductance and the resonant filter flow in the shunt capacitor. Not only can the Class E inverter operate at ZVS but also the voltage across the switch has a zero slope at the instant in which it is turned ON. This is referred to as ZDS. ZVS prevents the dissipation of the energy stored by the shunt capacitor when it turns on, and ZDS makes the circuit robust in the face of variations in the

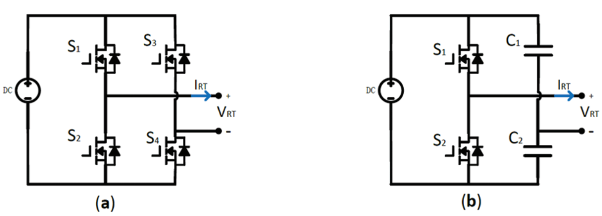

Fig. 8. (a) Full-bridge inverter and (b) half-bridge inverter.

components, frequency and switching instants (Diekhans and Doncker, 2015; Sokal and Sokal, 1975). However, owing to its resonant operation principle, the device voltage and current stress are relatively higher than that for a full- or half-bridge inverter, which threatens the reliability of the device. To ensure the circuit reliability when implemented in a WPT system where the load and coupling coefficient are always changing, a switch with a maximum voltage rating of at least four times the input voltage may be required. Therefore, Class E inverter is only suitable for low power and low voltage IPT systems (Trung et al., 2015; Casanova et al., 2009). Enhanced gallium nitride (eGaN) device is often adopted to enhance the delivered power in the MHz frequency region (Choi et al., 2018).

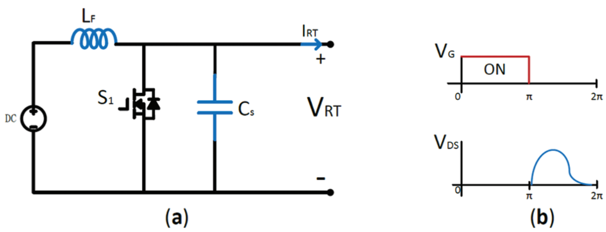

Fig. 9. (a) Class-E inverter topology before the resonant tank and (b) waveforms of V_G turning ON S_1 and its V_{DS}.

Latest research studies are focused on different methods in achieving high efficiency. For instance, controlling the phase-shift of the active rectifier, its output voltage level and modifying the equivalent secondary-side load impedance in Berger et al. (2015), it maximises the amount of extractable power in WPT system. In Hao et al. (2014), a 6 kW parallel power supply has been constructed by connecting three 2 kW power supplies in parallel obtaining a maximum efficiency of 94%. The system can also minimise uneven power-sharing, and it can continue to operate when a faulty parallel unit is electronically shut down. Aldhaher et al. (2014) found a way to compensate the effects of the misalignment on efficiency through a tuning scheme for the Class E inverter in transmission. The primary coil has a current-controlled method that allows the variable frequency to achieve optimum switching conditions regardless of the misalignment. Deng et al. (2017) created a prototype of a six-phase half-bridge parallel inverter for 20 kW WPT systems and achieving a 95.6% efficiency. Fu et al. (2014) designed a cascaded boost-buck DC–DC converter to provide the optimal impedance matching in 13.26-MHz WPT system for various loads including resistive load, ultra-capacitors and batteries achieving an overall system efficiency of 70%.

5. Further Developments in WPT System

5.1 Maximum efficiency tracking and modulation

In addition to the research studies mentioned above, it is important to notice that component tolerance and ageing of inductors and capacitors can also decrease the system efficiency. For this reason, many studies are now focused on how to track variation of the efficiency and maximise it when variation from the nominal value occurs. Mai et al. (2018) tracked the maximum efficiency under varied loads. An active single-phase rectifier (ASPR) with an auxiliary measurement coil (AMC) was also proposed reaching 91.7% efficiency loading 800 W. An integrated dynamic coupling factor estimation analysis by Dai et al. (2018) has been adopted to model the low coupling factor with an enhanced method for the maximum efficiency tracking. In Li et al. (2015b), the system efficiency is maximised efficiency while regulating the output voltage. Thanks to a constant operating frequency, the maximum efficiency point on the voltage trajectory is tracked dynamically. Similarly, at 6.78 MHz a loosely coupled series–series resonant coils were also effective to have the maximum efficiency in Yeo et al. (2017). Another method for automatic efficiency tracking created by Zhong and Hui (2015) used the switched-mode converter in the receiver module to emulate the optimum load. This method searches for the minimum input power point for a given output power.

In Zhong and Hui (2018), the same authors proposed a switched mode DC–DC converter in the receiver circuit and an ON–OFF keying modulation to emulate an equivalent load resistance over a wide range of power load. This simple and effective method, although with some switching losses, can be applied to any SS resonant WPT system. Lee at al. (2016b) used a multicycle Q-modulation that span across multiple carrier cycles. The system modulates the quality factor of the receiver coil and dynamically optimise the load to maximise the efficiency in two-coil system. In Li et al. (2018), it has been proposed a pulse density modulation (PDM) for maximum efficiency point tracking using the delta–sigma modulator with a dual-side soft switching. It is possible to avoid disadvantages of the complexity, power loss, hard switching, low average efficiency, DC voltage ripples and keep an efficiency over 70% in 0.5 m gap, which is 1.67 times the diameter of the coils.

5.2 Safety and security

In this part, we want to discuss the requirements for WPT systems that are becoming more important and will be developed in the next future. The improvement on transmission distance has guided the research in safety and security aspect is important. Questions about the safety of WPT system at home or stealing power from WPT sources are driving the research to some important points initially neglected. For this reason, more and more papers in the literature are focusing on safety and security improvements of WPT systems.

5.2.1 Safety

The human exposure to electric and magnetic fields in the transfer space must be considered in any WPT topology. The guideline for the level of electric field is 83 V/m and magnetic field is 21 A/m (Koohestani et al., 2017) recommended by the International Commission on Non-Ionizing Radiation Protection (ICNIRP) (Health Physics International Commission on Non-Ionizing Radiation Protection, 2010). Medium- and high-power WPT charging applications create high levels of field in the coils' proximity, then the safety of people nearby the charger becomes a fundamental requirement. In a 20 kW EV dynamic charger with transmitters of 0.5 m $\times$ 1.5 m in series (Cirimele et al., 2017), the authors pulsed the magnetic field (developed according to the ICNIRP guidelines) at the frequency of 85 kHz. Only if a vehicle is above them, the system will transfer power. At the same frequency, the authors of Laakso et al. (2014) investigated 7-kW WPT adopting a computational modelling to the electromagnetic field to humans. Jo et al. (2014) have been shown a variation of the pulse width to reduce harmonics and leakage. Furthermore, Choi et al. (2014b) presented three methods such as independent self-cancellation, the 3-dB dominant cancel method and the linkage free cancel method. In addition, the authors have reported other techniques, such as separating pickup rectifiers and magnetic mirror methods. Moreover, many shielding materials were presented, such as ferrite, metallic (aluminium) (Kim et al., 2014; Wen and Huang, 2016) and metamaterials (Besnoff et al., 2016; Cho et al., 2017).

5.2.2 Security

The power encryption in WPT was initially applied in Zhang et al. (2014b) and Zhang et al. (2015d). The encryption of power supply is based on the variation of transmitting frequency making out of resonance other not allowed receiver. A chaotic variation of the capacitor array based on algorithm the variation of the frequency and matching with the receiver for the maximum power delivered. Hence, the transmitted power can be packed with different frequencies and delivered to the receiver in a specified slot of time.

6. Conclusions

This paper presents an overview of the achievements in methods for enhancing efficiency and distance in WPT applications. The methods for improving the efficiency are based on increasing the efficiency of each block that a WPT system is included. Furthermore, the efficiency could be improved by correctly designing the coil, the compensation network for the resonance in the transmitter and receiver with other possible improvements in the power converter topology. Moreover, issues and methods for short, medium and long distances have been shown with an analytical consideration for the four-coil system.

Referring to the latest research, the progress of power control, compensation network topologies, coil designs, new artificial material and the overall performance of wireless transmission (such as the power level, efficiency, transfer distance, safety and security) are significantly improved. We hope that researchers and engineers will be inspired by these cutting-edge advances, promoting further upgrade in the development of WPT systems and accelerating the trading of this technique.

References

Abou Houran, M., Yang, X. and Chen, W. (2018). Magnetically Coupled Resonance WPT: Review of Compensation Topologies, Resonator Structures with Misalignment, and EMI Diagnostics. *Electronics,* 7, p. 296.

Ahmad, A., Alam, M. S. and Chabaan, R. (2018). A Comprehensive Review of Wireless Charging Technologies for Electric Vehicles. *IEEE Transactions on Transportation Electrification,* 4, pp. 38–63.

Ahn, D. and Hong, S. (2013). Effects of Coupling between Multiple Transmitters or Multiple Receivers on Wireless Power Transfer. *IEEE Transactions on Industrial Electronics,* 60, pp. 2602–2613.

Ahn, D. and Hong, S. (2014). A Transmitter or a Receiver Consisting of Two Strongly Coupled Resonators for Enhanced Resonant Coupling in Wireless Power Transfer. *IEEE Transactions on Industrial Electronics,* 61, pp. 1193–1203.

Aldhaher, S., Luk, P. C. K. and Whidborne, J. F. (2014). Electronic Tuning of Misaligned Coils in Wireless Power Transfer Systems. *IEEE Transactions on Power Electronics,* 29, pp. 5975–5982.

Almasoud, A. H. and Gandayh, M. H. (2015). Future of Solar Energy in Saudi Arabia. *Journal of King Saud University – Engineering Sciences,* 27, pp. 153–157, 1018–3639.

Alphones, A. and Sampath, J. P. K. (2015). Metamaterial assisted wireless power transfer system. In: *Proceedings of the Asia-Pacific Microwave Conference*, pp. 1–3.

Balanis, C. A. (2005). *Chapter 3. In Antenna Theory: Analysis and Design*, 3rd ed. Hoboken, NJ: John Wiley & Sons, Inc.

Barman, S. D., Reza, A. W., Kumar, N., Karim, M. E. and Munir, A. B. (2015). Wireless Powering by Magnetic Resonant Coupling: Recent Trends in Wireless Power Transfer System and its Applications. *Renewable and Sustainable Energy Reviews,* 51, pp. 1525–1552.

Berger, A., Agostinelli, M., Vesti, S., Oliver, J. A., Cobos, J. A. and Huemer, M. (2015). A Wireless Charging System Applying Phase-Shift and Amplitude Control to Maximize Efficiency and Extractable Power. *IEEE Transactions on Power Electronics,* 30, pp. 6338–6348.

Besnoff, J., Chabalko, M. and Ricketts, D. S. (2016). A Frequency-Selective Zero-Permeability Metamaterial Shield for Reduction of Near-Field Electromagnetic Energy. *IEEE Antennas and Wireless Propagation Letters,* 15, pp. 654–657.

Bilotti, F. and Sevgi, L. (2012). Metamaterials: Definitions, Properties, Applications, and FDTD-Based Modeling and Simulation. *International Journal of RF and Microwave Computer-Aided Engineering,* 22, pp. 422–438.

Bosshard, R. and Kolar, J. W. (2016). Inductive Power Transfer for Electric Vehicle Charging: Technical Challenges And Tradeoffs. *IEEE Power Electronics Magazine,* 3, pp. 22–30.

C.R Nave Georgia State University. (2001). *Magnetic Properties of Ferromagnetic Materials*. Retrieved 2013-12-01.

Cabrera, F. L. and De Sousa, F. R. (2016). Achieving Optimal Efficiency in Energy Transfer to a CMOS Fully Integrated Wireless Power Receiver. *IEEE Transactions on Microwave Theory and Techniques,* 64, pp. 3703–3713.

Campi, T., Cruciani, S., Palandrani, F., Santis, V. D., Hirata, A. and Feliziani, M. (2016). Wireless Power Transfer Charging System for AIMDs and Pacemakers. *IEEE Transactions on Microwave Theory and Techniques,* 64, pp. 633–642.

Campi, T., Cruciani, S., Santis, V. D., Maradei, F. and Feliziani, M. (2018). Feasibility study of a wireless power transfer system applied to a leadless pacemaker. *IEEE Wireless Power Transfer Conference (WPTC)*, Montreal, QC, Canada: IEEE, pp. 1–4.

Cannon, B. L., Hoburg, J. F., Stancil, D. and Goldstein, S. C. (2009). Magnetic Resonant Coupling as a Potential Means for Wireless Power Transfer to Multiple Small Receivers. *IEEE Transactions on Power Electronics,* 24, pp. 1819–1825.

Casanova, J. J., Low, Z. N. and Lin, J. (2009). Design and Optimization of a Class-E Amplifier for a Loosely Coupled Planar Wireless Power System. *IEEE Transactions on Circuits and Systems II: Express Briefs,* 56, pp. 830–834.

Chabalko, M. J. and Sample, A. P. (2014). Resonant Cavity Mode Enabled Wireless Power Transfer. *Applied Physics Letters,* 105, p. 243902. AIP Publishing.

Chabalko, M. J. and Sample, A. P. (2015). Three-Dimensional Charging via Multimode Resonant Cavity Enabled Wireless Power Transfer. *IEEE Transactions on Power Electronics,* 30, pp. 6163–6173.

Charthad, J., Weber, M. J., Chang, T. C. and Arbabian, A. (2015). A mm-Sized Implantable Medical Device (IMD) with Ultrasonic Power Transfer and a Hybrid

Bi-Directional Data Link. *IEEE Journal of Solid-State Circuits,* 50, pp. 1741–1753.

Chen, K. and Zhao, Z. (2013). Analysis of the Double-Layer Printed Spiral Coil for Wireless Power Transfer. *IEEE Journal of Emerging and Selected Topics in Power Electronics,* 1, pp. 114–121.

Chen, L., Liu, S., Zhou, Y. C. and Cui, T. J. (2013). An Optimizable Circuit Structure for High-Efficiency Wireless Power Transfer. *IEEE Transactions on Industrial Electronics,* 60, pp. 339–349.

Ching, T. W. and Wong, Y. S. (2013). Review of wireless charging technologies for electric vehicles. In: *5th International Conference on Power Electronics Systems and Applications (PESA)*, pp. 1–4.

Cho, Y., Kim, J. J., Kim, D. H., Lee, S., Kim, H., Song, C., et al. (2016). Thin PCB-Type Metamaterials for Improved Efficiency and Reduced EMF Leakage in Wireless Power Transfer Systems. *IEEE Transactions on Microwave Theory and Techniques,* 64, pp. 353–364.

Cho, Y., Lee, S., Kim, D. H., Kim, H., Song, C., Kong, S., et al. (2017). Thin Hybrid Metamaterial Slab with Negative and Zero Permeability for High Efficiency and Low Electromagnetic Field in Wireless Power Transfer Systems. *IEEE Transactions on Electromagnetic Compatibility,* 60, pp. 1001–1009.

Choi, B. H., Lee, E. S., Kim, J. H. and Rim, C. T. (2014a). 7m-off-long-distance extremely loosely coupled inductive power transfer systems using dipole coils. In: *IEEE Energy. Conversion Congress and Expo (ECCE)*, pp. 858–563.

Choi, B. H., Lee, E. S., Sohn, Y. H., Jang, G. C. and Rim, C. T. (2016). Six Degrees of Freedom Mobile Inductive Power Transfer by Crossed Dipole Tx and Rx Coils. *IEEE Transactions on Power Electronics,* 31, pp. 3252–3272.

Choi, J. and Seo, C. H. (2010). High-Efficiency Wireless Energy Transmission Using Magnetic Resonance Based on Negative Refractive Index Metamaterial. *Progress in Electromagnetics Research,* 106, pp. 33–47.

Choi, J., Tsukiyama, D., Tsuruda, Y. and Davila, J. M. R. (2018). High-Frequency, High-Power Resonant Inverter with eGaN FET for Wireless Power Transfer. *IEEE Transactions on Power Electronics,* 33, pp. 1890–1896.

Choi, S. Y., Gu, B. W., Jeong, S. Y. and Rim, C. T. (2015). Advances in Wireless Power Transfer Systems for Roadway-Powered Electric Vehicles. *IEEE Journal of Emerging and Selected Topics in Power Electronics,* 3, pp. 18–36.

Choi, S. Y., Gu, B. W., Lee, S. W., Lee, W. Y., Huh, J. and Rim, C. T. (2014b). Generalized Active EMF Cancel Methods for Wireless Electric Vehicles. *IEEE Transactions on Power Electronics,* 29, pp. 5770–5783.

Cirimele, V., Freschi, F., Giaccone, L., Pichon, L. and Repetto, M. (2017). Human Exposure Assessment in Dynamic Inductive Power Transfer for Automotive Applications. *IEEE Transactions on Magnetics,* 53, pp. 1–4.

Cullity, B. D. and Graham, C. D. (2008). *Introduction to Magnetic Materials*, 2nd ed. p. 568, 16.

Dai, J. and Ludois, D. C. (2015). A Survey of Wireless Power Transfer and a Critical Comparison of Inductive and Capacitive Coupling for Small Gap Applications. *IEEE Transactions on Power Electronics,* 30, pp. 6017–6029.

Dai, X., Li, X., Li, Y. and Hu, P. (2018). Maximum Efficiency Tracking for Wireless Power Transfer Systems with Dynamic Coupling Coefficient Estimation. *IEEE Transactions on Power Electronics,* 33, pp. 5005–5015.

Deng, J., Li, W., Nguyen, T. D., Li, S. and Mi, C. C. (2015). Compact and Efficient Bipolar Coupler for Wireless Power Chargers: Design and Analysis. *IEEE Transactions on Power Electronics,* 30, pp. 6130–6140.

Deng, Q. J., Liu, J. T., Czarkowski, D., Hu, W. S. and Zhou, H. (2017). An Inductive Power Transfer System Supplied by a Multiphase Parallel Inverter. *IEEE Transactions on Industrial Electronics,* 64, pp. 7039–7048.

Diekhans, T. and Doncker, R. W. D. (2015). A Dual-Side Controlled Inductive Power Transfer System Optimized for Large Coupling Factor Variations and Partial Load. *IEEE Transactions on Power Electronics,* 30, pp. 6320–6328.

Elnail, K. E. I., Huang, X., Xiao, C., Tan, L. and Haozhe, X. (2018). Core Structure and Electromagnetic Field Evaluation in WPT Systems for Charging Electric Vehicles. *Energies,* 11, p. 1734.

Etemadrezaei, M. and Lukic, S. M. (2016). Coated-Strand Litz Wire For Multi-Megahertz Frequency Applications. *IEEE Transactions on Magnetics,* 52, pp. 1–11.

Fakidis, J., Videv, S., Kucera, S., Claussen, H. and Haas, H. (2016). Indoor Optical Wireless Power Transfer to Small Cells at Nighttime. *Journal of Lightwave Technology,* 34, pp. 3236–3258.

Feng, H., Cai, T., Duan, S., Zhao, J., Zhang, X. and Chen, C. (2016). An LCC Compensated Resonant Converter Optimized for Robust Reaction to Large Coupling Variation in Dynamic Wireless

Power Transfer. *IEEE Transactions on Industrial Electronics,* 63, pp. 6591–6601.
Fu, M., Ma, C. and Zhu, X. (2014). A Cascaded Boost-Buck Converter for High Efficiency Wireless Power Transfer Systems. *IEEE Transactions on Industrial Informatics,* 10, pp. 1972–1980.
Galbraith, D. C., Soma, M. and White, R. L. (1987). A Wide-Band Efficient Inductive Transdennal Power and Data Link with Coupling Insensitive Gain. *IEEE Transactions on Biomedical Engineering,* 34, pp. 265–275.
Garnica, J., Chinga, R. A. and Lin, J. (2013). Wireless Power Transmission: From Far Field to Near Field. *Proceedings of the IEEE,* 101, pp. 1321–1331.
Grover, F. W. (2004). *Inductance Calculations: Working Formulas and Tables*. Washington, DC, USA: Courier Corporation.
Hadadtehrani, P., Kamalinejad, P., Molavi, R. and Mirabbasi, S. (2016). On the use of conical helix inductors in wireless power transfer systems. In: *Proceedings of the IEEE Canadian Conference on Electrical and Computer Engineering (CCECE)*, pp. 1–4.
Hao, H., Covic, G. A. and Boys, J. T. (2014). A Parallel Topology for Inductive Power Transfer Power Supplies. *IEEE Transactions on Power Electronics,* 29, pp. 1140–1151.
Health Physics International Commission on Non-Ionizing Radiation Protection. (2010). *Guidelines for Limiting Exposure to Time-Varying Electric and Magnetic Fields (1Hz to 100kHz)*. 99, pp. 818–836.
Ho, J. S., Kim, S. and Poon, A. S. Y. (2013). Midfield Wireless Powering for Implantable Systems. *Proceedings of the IEEE,* 101, pp. 1369–1378.
Hoang, H. and Bien, F. (2012). Maximizing Efficiency of Electromagnetic Resonance Wireless Power Transmission Systems with Adaptive Circuits. *InTech Open Access,* pp. 207–225.
Holmer, N. G. and Lindstrom, K. (1973). Highly Isolated Power Supply Energized by Ultrasound. *Journal of Medical and Biological Engineering,* 11, pp. 233–235.
Hou, J., Chen, Q., Wong, S. C., Tse, C. K. and Ruan, X. (2015). Analysis and Control of Series/Series-Parallel Compensated Resonant Converter for Contactless Power Transfer. *IEEE Journal of Emerging and Selected Topics in Power Electronics,* 3, pp. 124–136.
Huh, J., Lee, S. W., Lee, W. Y., Cho, G. H. and Rim, C. T. (2011). Narrow-Width Inductive Power Transfer System for Online Electrical Vehicles. *IEEE Transactions on Power Electronics,* 26, pp. 3666–3679.
Hui, S. Y. R., Zhong, W. and Lee, C. K. (2014). A Critical Review of Recent Progress in Mid-Range Wireless Power Transfer. *IEEE Transactions on Power Electronics,* 9, pp. 4500–4511.
Hwang, K., Cho, J., Kim, D., Park, J., Kwon, J. K., Kwak, S. I., et al. (2014). An Autonomous Coil Alignment System for the Dynamic Wireless Charging of Electric Vehicles to Minimize Lateral Misalignment. *Energies,* 10, p. 315.
Jarvis, S., Mukherjee, J., Perren, M. and Sweeney, J. S. (2013). On the fundamental efficiency limits of photovoltaic converters for optical power transfer applications. *39th IEEE Photovoltaic Specialists Conference (PVSC)*, IEEE, pp. 1031–1035.
Jawad, A. M., Nordin, R. G., Sadik, K., Jawad, H. M., Ismail, M. and Abu-AlShaeer, M. J. (2018). Single-Tube and Multi-Turn Coil Near-Field Wireless Power Transfer for Low-Power Home Appliances. *Energies,* 11, p. 1969.
Jeong, I. S., Jung, B. I., You, D. S. and Choi, H. S. (2016). Analysis of S-Parameters in Magnetic Resonance WPT Using Superconducting Coils. *IEEE Transactions on Applied Superconductivity,* 26, pp. 1–4.
Jiang, C., Chau, K. T., Ching, T. W., Liu, C. and Han, W. (2017b). Time-Division Multiplexing Wireless Power Transfer for Separately Excited DC Motor Drives. *IEEE Transactions on Magnetics,* 53, pp. 1–5.
Jiang, C., Chau, K. T., Liu, C. and Lee, C. H. T. (2017a). An Overview of Resonant Circuits for Wireless Power Transfer. *Energies,* 10, p. 894.
Jo, M., Sato, Y., Kaneko, Y. and Abe, S. (2014). Methods for reducing leakage electric field of a wireless power transfer system for electric vehicles. In: *Proceedings of the IEEE Energy Conversion Congress and Exposition (ECCE)*, pp. 1762–1769.
Jolani, F., Yu, Y. and Chen, Z. (2014). A Planar Magnetically Coupled Resonant Wireless Power Transfer System Using Printed Spiral Coils. *IEEE Antennas and Wireless Propagation Letters,* 13, pp. 1648–1651.
Jonah, O., Georgakopoulos, S. V. and Tentzeris, M. M. (2013). Orientation insensitive power transfer by magnetic resonance for mobile devices. In: *IEEE Wireless Power Transfer*, pp. 5–8.
Kan, T., Nguyen, T. D., White, J. C., Malhan, R. K. and Mi, C. C. (2017). A New Integration Method for an Electric Vehicle Wireless Charging System Using LCC Compensation Topology: Analysis and Design. *IEEE Transactions on Power Electronics,* 32, pp. 1638–1650.

Kazmierkowski, M. P. and Moradewicz, A. J. (2012). Unplugged but Connected: Review of Contactless Energy Transfer Systems. *IEEE Industrial Electronics Magazine,* 6, pp. 47–55.

Khan, I., Qureshi, M. I., Rehman, M. U. and Khan, W. T. (2017). Long range wireless power transfer via magnetic resonance. In: *Progress in Electromagnetics Research Symposium - Fall (PIERS - FALL)*, pp. 3079–3085.

Kim, D., Abu-Siada, A. and Sutinjo, A. (2018). State-of-the-Art Literature Review of WPT: Current Limitations and Solutions on IPT. *Electric Power Systems Research,* 154, pp. 493–502, 0378–7796.

Kim, J., Kim, H., Song, C., Kim, I. M., Kim, Y. and Kim, J. (2014). Electromagnetic interference and radiation from wireless power transfer systems. In: *Proceedings of the International Symposium on Electromagnetic Compatibility (EMC)*, pp. 171–176.

Kim, K. Y. (2009). Comparative Analysis of Guided Modal Properties of Double Positive and Double-Negative Meta-Material Slab Waveguides. *Radio Engineering,* 18, pp. 17–123.

Kim, M., Kim, H., Kim, D., Jeong, Y., Park, H. H. and Ahn, S. (2015a). A Three-Phase Wireless-Power-Transfer System for Online Electric Vehicles with Reduction of Leakage Magnetic Fields. *IEEE Transactions on Microwave Theory and Techniques,* 63, pp. 3806–3813.

Kim, S., Jung, D. H., Kim, J. J., Bae, B., Kong, S., Ahn, S., et al. (2015b). High-Efficiency PCB-and Package-Level Wireless Power Transfer Interconnection Scheme Using Magnetic Field Resonance Coupling. *IEEE Transactions on Components, Packaging and Manufacturing Technology,* 5, pp. 863–878.

Kim, Y. H., Kang, S. Y., Cheon, S., Lee, M. L. and Zyung, T. (2010). Wireless power transmission to multi devices through resonant coupling. *Proceedings of the International Conference on Electronics Machine System*, pp. 2000–2002.

Kimmich, H. P. (1982). Biotelemetry, Based on Optical Transmission. *Biotelemetry and Patient Monitoring,* 9, pp. 129–143.

Ko, Y. D. and Jang, Y. J. (2013). The Optimal System Design of the Online Electric Vehicle Utilizing Wireless Power Transmission Technology. *IEEE Transactions on Intelligent Transportation Systems,* 2013, pp. 1255–1265.

Koohestani, M., Zhadobov, M. and Ettorre, M. (2017). Design Methodology of a Printed WPT System for HF-Band Mid-Range Applications Considering Human Safety Regulations. *IEEE Transactions on Microwave Theory and Techniques,* 65, pp. 270–279.

Kurs, A., Karalis, A., Moffatt, R., Joannopoulos, J. D., Fisher, P. and Soljacic, M. (2007). Wireless Power Transfer via Strongly Coupled Magnetic Resonances. *Science,* 317, pp. 83–86.

Kurs, A., Moffatt, R. and Solijacic, M. (2010). Simultaneous Mid-Range Power Transfer to Multiple Devices. *Applied Physics Letters,* 96, p. 044102. American Institute of Physics (AIP)

Laakso, I., Hirata, A. and Fujiwara, O. (2014). Computational dosimetry for wireless charging of an electrical vehicle. In: *Proceedings of the International Symposium on Electromagnetic Compatibility (EMC)*, pp. 202–205.

Lee, B., Yeon, P. and Ghovanloo, M. (2016b). A Multi-Cycle Q-Modulation for Dynamic Optimization of Inductive Links. *IEEE Transactions on Industrial Electronics,* 63, pp. 5091–5100.

Lee, K. and Cho, D. H. (2013). Diversity Analysis of Multiple Transmitters in Wireless Power Transfer System. *IEEE Transactions on Magnetics,* 49, pp. 2946–2952.

Lee, S. H. and Lorenz, R. D. (2013). Surface spiral coil design methodologies for high efficiency high power low flux density large air-gap wireless power transfer systems. In: *IEEE Applied Power Electronics Conference and Expo (APEC)*, pp. 1783–1790.

Lee, S. H., Lee, B. S. and Lee, J. H. (2016a). A New Design Methodology for a 300-kW, Low Flux Density, Large Air Gap, Online Wireless Power Transfer System. *IEEE Transactions on Industry Applications,* 52, pp. 4234–4242.

Lee, W. S., Son, W. I., Oh, K. S. and Yu, J. W. (2015). Contactless Energy Transfer Systems Using Antiparallel Resonant Loops. *IEEE Transactions on Industrial Electronics,* 60, pp. 350–359.

Li, H. C., Li, J., Wang, K. P., Chen, W. J. and Yang, X. (2015b). A Maximum Efficiency Point Tracking Control Scheme for Wireless Power Transfer Systems Using Magnetic Resonant Coupling. *IEEE Transactions on Power Electronics,* 30, pp. 3998–4008.

Li, H., Fang, J., Chen, S., Wang, K. and Tang, Y. (2018). Pulse Density Modulation for Maximum Efficiency Point Tracking of Wireless Power Transfer Systems. *IEEE Transactions on Power Electronics,* 33, pp. 5492–5501.

Li, S., Li, W., Deng, J., Nguyen, T. D. and Mi, C. C. (2014). A Double-Sided LCC Compensation Network and its Tuning Method for Wireless Power Transfer.

IEEE Transactions on Vehicular Technology, 64, pp. 2261–2273.

Li, W., Zhao, H., Deng, J., Li, S. and Mi, C. C. (2016). Comparison Study on SS and Double-Sided LCC Compensation Topologies for EV/PHEV Wireless Chargers. *IEEE Transactions on Vehicular Technology,* 65, pp. 4429–4439.

Li, W., Zhao, H., Li, S., Deng, J., Kan, T. and Mi, C. C. (2015a). Integrated LCC Compensation Topology for Wireless Charger in Electric and Plug-in Electric Vehicles. *IEEE Transactions on Industrial Electronics,* 62, pp. 4215–4225.

Lim, Y., Tang, H., Lim, S. and Park, J. (2014). An Adaptive Impedance-Matching Network Based on a Novel Capacitor Matrix for Wireless Power Transfer. *IEEE Transactions on Power Electronics,* 29, pp. 4403–4413.

Liu, F., Zhang, Y., Chen, K., Zhao, Z. and Yuan, L. (2016). A comparative study of load characteristics of resonance types in wireless transmission systems. In: *Proceedings of the IEEE Asia-Pacific International Symposium on Electromagnetic Compatibility (APEMC)*, Vol. 1, pp. 203–206.

Liu, Y., Li, B., Huang, M., Chen, Z. and Zhang, X. (2018). An Overview of Regulation Topologies in Resonant Wireless Power Transfer Systems for Consumer Electronics or Bio-Implants. *Energies,* 11, p. 1737.

Low, Z. N., Chinga, R. A., Tseng, R. and Lin, J. (2009). Design and Test of a High-Power High-Efficiency Loosely Coupled Planar Wireless Power Transfer System. *IEEE Transactions on Industrial Electronics,* 56, pp. 1801–1812.

Lu, F., Zhang, H., Hofmann, H. and Mi, C. C. (2016). A Dynamic Charging System with Reduced Output Power Pulsation for Electric Vehicles. *IEEE Transactions on Industrial Electronics,* 63, pp. 6580–6590.

Madawala, U. K. and Thrimawithana, D. J. (2011). A Bidirectional Inductive Power Interface for Electric Vehicles in V2G Systems. *IEEE Transactions on Industrial Electronics,* 58, pp. 4789–4796.

Mai, R. K., Liu, Y. R., Li, Y., Yue, P. F., Cao, G. Z. and He, Z. Y. (2018). An Active Rectifier-Based Maximum Efficiency Tracking Method Using an Additional Measurement Coil for Wireless Power Transfer. *IEEE Transactions on Power Electronics,* 33, pp. 716–728.

Marian, V., Allard, B., Vollaire, C. and Verdier, J. (2012). Strategy for Microwave Energy Harvesting from Ambient Field or a Feeding Source. *IEEE Transactions on Power Electronics,* 27, pp. 4481–4491.

Market Research Future. (2019). *Wireless Power Transmission Market 2019 Global Industry Size, Growth, Emerging Technologies, Competitive Landscape, Opportunities, Segmentation, Future Trends and Regional Forecast 2022.* Global Wireless Power Transmission Market Research Report- Forecast 2022 Market Analysis, Scope, Stake, Progress, Trends and Forecast to 2022. Available at: https://www.marketwatch.com/press-release/wireless-power-transmission-market-2019-global-industry-size-growth-emerging-technologies-competitive-landscape-opportunities-segmentation-future-trends-and-regional-forecast-2022-2019-03-12 [Accessed 3 Sept 2019].

Markets and Markets. (2019). *Market Research Report*. Available at: https://www.marketsandmarkets.com/PressReleases/wireless-power-transmission.asp [Accessed 13 Jan 2019]

Mei, H., Huang, Y. W., Thackston, K. A. and Irazoqui, P. P. (2016). Optimal Wireless Power Transfer to Systems in an Enclosed Resonant Cavity. *IEEE Antennas and Wireless Propagation Letters,* 15, pp. 1036–1039.

Mei, H., Thackston, K. A., Bercich, R. A., Jefferys, J. G. and Irazoqui, P. P. (2017). Cavity Resonator Wireless Power Transfer System for Freely Moving Animal Experiments. *IEEE Transactions on Biomedical Engineering,* 64, pp. 775–785.

Miller, J. M., Onar, O. C. and Chinthavali, M. (2015). Primary-Side Power Flow Control of Wireless Power Transfer for Electric Vehicle Charging. *IEEE Journal of Emerging and Selected Topics in Power Electronics,* 3, pp. 147–162.

Mirbozorgi, S. A., Yeon, P. and Ghovanloo, M. (2017). Robust Wireless Power Transmission to mm-Sized Free-Floating Distributed Implants. *IEEE Transactions on Biomedical Circuits and Systems,* 11, pp. 692–702.

Mohan, S. S. (1999). *The Design, Modeling and Optimization of On-Chip Inductor and Transformer Circuits.* Ph.D. Thesis. Stanford, CA, USA: Stanford University.

Moon, S. and Moon, G. W. (2016). Wireless Power Transfer System with an Asymmetric Four-Coil Resonator for Electric Vehicle Battery Chargers. *IEEE Transactions on Power Electronics,* 31, pp. 6844–6854.

Mur-Miranda, J. O., Fanti, G., Feng, Y., Omanakuttan, K., Ongie, R., Setjoadi, A., et al. (2010). Wireless power transfer using weakly coupled magneto-static resonators. In: *Proceedings of the IEEE ECCE*, pp. 4179–4186.

Musavi, F. and Eberle, W. (2014). Overview of Wireless Power Transfer Technologies for Electric Vehicle Battery Charging. *IET Power Electronics,* 7, pp. 60–66.

Nguyen, V. T., Yu, S., Yim, S. and Park, K. (2017). Optimizing compensation topologies for inductive power transfer at different mutual inductances. In: *IEEE PELS Workshop on Emerging Technologies: Wireless Power Transmission (WoW)*, pp. 153–156.

Oh, T. and Lee, B. (2013). Analysis of Wireless Power Transfer Using Metamaterial Slabs Made of Ring Resonators at 13.56 MHz. *Journal of Electromagnetic Engineering and Science,* 13, pp. 259–262.

Onar, O. C., Miller, J. M., Campbell, S. L., Coomer, C., White, C. P. and Seiber, L. E. (2013). A novel wireless power transfer for in-motion EV/PHEV charging. In: *Proceedings of the IEEE Applied Power Electronics Conference Exposition (APEC)*, pp. 3073–3080.

Park, C., Lee, S., Cho, G. H. and Rim, C. T. (2015). Innovative 5-m-Off-Distance Inductive Power Transfer Systems with Optimally Shaped Dipole Coils. *IEEE Transactions on Power Electronics,* 30, pp. 817–827.

Park, J., Tak, Y., Kim, Y., Kim, Y. and Nam, S. (2011). Investigation of Adaptive Matching Methods for Near-Field Wireless Power Transfer. *IEEE Transactions on Antennas and Propagation,* 59, pp. 1769–1773.

Park, M., Nguyen, V. T., Yu, S. D., Yim, S. W., Park, K., Min, B. D., et al. (2016). A study of wireless power transfer topologies for 3.3 kW and 6.6 kW electric vehicle charging infrastructure. In: *Proceedings of the IEEE Transportation Electrification Conference and Expo (ITEC Asia-Pacific)*, pp. 689–692.

Patil, D., McDonough, M. K., Miller, J. M., Fahimi, B. and Balsara, P. T. (2018). Wireless Power Transfer for Vehicular Applications: Overview and Challenges. *IEEE Transactions on Transportation Electrification,* 4, pp. 3–37.

Pinuela, M., Yates, D. C., Lucyszyn, S. and Mitcheson, P. D. (2013). Maximizing DC-to-Load Efficiency for Inductive Power Transfer. *IEEE Transactions on Power Electronics,* 28, pp. 2437–2447.

Qu, X., Jing, Y., Han, H., Wong, S. C. and Tse, C. K. (2017). Higher Order Compensation for Inductive-Power-Transfer Converters with Constant-Voltage or Constant-Current Output Combating Transformer Parameter Constraints. *IEEE Transactions on Power Electronics,* 32, pp. 394–405.

Raab, F. H. (1978). Effects of Circuit Variations on the Class E Tuned Power Amplifier. *IEEE Journal of Solid-State Circuits,* 13, pp. 239–247.

RamRakhyani, A. K. and Lazzi, G. (2013). On the Design of Efficient Multi-Coil Telemetry System for Biomedical Implants. *IEEE Transactions on Biomedical Circuits and Systems,* 7, p. 11.

Ranaweera, A., Duong, T. P., Lee, B. S. and Lee, J. K. (2014). Experimental investigation of 3D metamaterial formid-range wireless power transfer. In: *Proceedings of the IEEE Wireless Power Transfer Conference*, pp. 92–95.

Reatti, A., Corti, F. and Pugi, L. (2018). Wireless power transfer for static railway applications. In: *IEEE International Conference on Environment and Electrical Engineering/IEEE Industrial and Commercial Power System Europe (EEEIC/I&CPS Europe)*, pp. 1–6.

Relative Permeability Hyperphysics. (2008). *Hyperphysics.phy-astr.gsu.edu*. Retrieved 2011-11-08.

Samanta, S. and Rathore, A. K. (2015). A New Current-Fed CLC Transmitter and LC Receiver Topology for Inductive Wireless Power Transfer Application: Analysis, Design, and Experimental Results. *IEEE Transactions on Transportation Electrification,* 1, pp. 357–368.

Sample, A. P., Meyer, D. T. and Smith, J. R. (2011). Analysis, Experimental Results, and Range Adaptation of Magnetically Coupled Resonators for Wireless Power Transfer. *IEEE Transactions on Industrial Electronics,* 58, pp. 544–554.

Sandoval, F. S., Delgado, S. M., Moazenzadeh, A. and Wallrabe, U. (2017). Nulls-Free Wireless Power Transfer with Straightforward Control of Magneto Inductive Waves. *IEEE Transactions on Microwave Theory and Techniques,* 65, pp. 1087–1093.

Sato, M., Yamamoto, G., Gunji, D., Imura, T. and Fujimoto, H. (2016). Development of Wireless In-Wheel Motor Using Magnetic Resonance Coupling. *IEEE Transactions on Power Electronics,* 31, pp. 5270–5278.

Seo, D. W., Lee, J. H. and Lee, H. S. (2016). Optimal Coupling to Achieve Maximum Output Power in a WPT System. *IEEE Transactions on Industrial Electronics,* 31, pp. 3994–3998.

Shekhar, A., Prasanth, V., Bauer, P. and Bolech, M. (2016). Economic Viability Study of an On-Road Wireless Charging System with a Generic Driving Range Estimation Method. *Energies,* 9, p. 76.

Shin, J., Shin, S., Kim, Y., Ahn, S., Lee, S., Jung, G., et al. (2014). Design and Implementation of Shaped Magnetic-Resonance-Based Wireless Power

Transfer System for Roadway-Powered Moving Electric Vehicles. *IEEE Transactions on Industrial Electronics,* 61, pp. 1179–1192.

Sokal, N. O. (1998). Class E High-Efficiency Power Amplifiers, from HF to Microwave. *IEEE MTT-S International Microwave Symposium Digest,* 2, pp. 1109–1112.

Sokal, N. O. and Sokal, A. D. (1975). Class E-A New Class of High-Efficiency Tuned Single-Ended Switching Power Amplifiers. *IEEE Journal of Solid-State Circuits,* 10, pp. 168–176.

Song, J., Kim, S., Bae, B., Kim, J. J., Jung, D. H. and Kim, J. (2014). Design and analysis of magnetically coupled coil structures for PCB-to-active interposer wireless power transfer in 2.5 D/3D-IC. In: *Proceedings of the IEEE Electrical Design of Advanced Packaging and System Symposium (EDAPS)*, pp. 1–4.

Sullivan, C. R. (2013). Layered foil as an alternative to Litz wire: multiple methods for equal current sharing among layers. In: *Workshop on Control and Modeling for Power Electronics (COMPEL)*.

Tampubolon, M., Pamungkas, L., Chiu, H. J., Liu, Y. C. and Hsieh, Y. C. (2018). Dynamic Wireless Power Transfer for Logistic Robots. *Energies,* 11, p. 527.

Theodoridis, M. P. (2012). Effective Capacitive Power Transfer. *IEEE Transactions on Power Electronics,* 27, pp. 4906–4913.

Thompson, M. C. (1991). *Inductance Calculation Techniques-Part II: Approximations and Handbook Methods*. University Park, PA, USA: CiteSeer.

Trung, N. K., Ogata, T., Tanaka, S. and Akatsu, K. (2015). PCB design for 13.56MHz half-bridge class D inverter for wireless power transfer system. *9th International Conference on Power Electronics – ECCE Asia (ICPE-ECCE Asia)*, pp. 1692–1699.

Tsuji, T., Fujimoto, T., Izuto, T. and Togawa, T. (1993). Telemetry of organ temperature with quartz crystal resonator using ultrasonic detection for preoperative patient monitoring. *Proceedings of the 12th International Symposium Biotel*, IEEE, pp. 378–380.

Umenei, A. E. (2019). *Understanding Low Frequency Non-Radiative Power Transfer*. Available at: https://www.wirelesspowerconsortium.com [Accessed 13 Jan 2019].

Villa, J. L., Sallan, J., Osorio, J. F. S. and Llombart, A. (2012). High-Misalignment Tolerant Compensation Topology for ICPT Systems. *IEEE Transactions on Industrial Electronics,* 59, pp. 945–951.

Wang, B. and Teo, K. H. (2012). Metamaterials for wireless power transfer. *Proceedings of the IEEE International Workshop Antenna Technology*, pp. 161–164.

Wang, C. S., Covic, G. A. and Stielau, O. H. (2004). Investigating an LCL Load Resonant Inverter for Inductive Power Transfer Applications. *IEEE Transactions on Power Electronics,* 19, pp. 995–1002.

Wang, C. S., Stielau, O. H. and Covic, G. A. (2005). Design Considerations for a Contactless Electric Vehicle Battery Charger. *IEEE Transactions on Industrial Electronics,* 52, pp. 1308–1314.

Wang, Y. F., Yang, L., Wang, C. S., Li, W., Qie, W. and Tu, S. J. (2015). High Step-Up 3-Phase Rectifier with Fly-Back Cells and Switched Capacitors for Small-Scaled Wind Generation Systems. *Energies,* 8, pp. 2742–2768.

Wang, Y., Yao, Y., Liu, X. and Xu, D. (2017). S/CLC Compensation Topology Analysis and Circular Coil Design for Wireless Power Transfer. *IEEE Transactions on Transportation Electrification,* 3, pp. 496–507.

Wang, Z., Wei, X. and Dai, H. (2016). Design and Control of a 3 kW Wireless Power Transfer System for Electric Vehicles. *Energies,* 9, p. 10.

Wei, X., Wang, Z. and Dai, H. (2014). A Critical Review of Wireless Power Transfer via Strongly Coupled Magnetic Resonances. *Energies*, 7(7), pp. 4316–4341.

Wen, F. and Huang, X. (2016). Optimal Magnetic Field Shielding Method by Metallic Sheets in Wireless Power Transfer System. *Energies,* 9, p. 733.

Wu, H. H., Gilchrist, A., Sealy, K. and Bronson, D. (2012a). A 90 percent efficient 5 kW inductive charger for EVs. In: *Proceedings of IEEE Energy Conversion Congress and Exposition*, pp. 275–282.

Wu, H. H., Gilchrist, A., Sealy, K. D. and Bronson, D. (2012b). A High Efficiency 5 kW Inductive Charger for EVs Using Dual Side Control. *IEEE Transactions on Industrial Informatics,* 8, pp. 585–595.

Wu, J., Wang, B., Yerazunis, W. S. and Teo, K. H. (2013). Wireless power transfer with artificial magnetic conductors. In: *Proceedings of the IEEE Wireless Power Transmission Conference*, pp. 155–158.

Yang, C. and Tsunekawa, K. (2014). A novel parallel double helix loop resonator for magnetic coupled resonance wireless power transfer. In: *PIERS Proceedings*, pp. 466–470.

Yang, Y., El Baghdadi, M., Lan, Y., Benomar, Y., Van Mierlo, J. and Hegazy, O. (2018). Design Methodology, Modeling, and Comparative Study of Wireless Power Transfer Systems for Electric Vehicles. *Energies,* 11, p. 1716.

Yeo, T. D., Kwon, D., Khang, S. T. and Yu, J. W. (2017). Design of Maximum Efficiency Tracking Control Scheme for Closed-Loop Wireless Power Charging System Employing Series Resonant Tank. *IEEE Transactions on Power Electronics,* 32, pp. 471–478.

Yi, Y., Buttner, U., Fan, Y. and Foulds, I. G. (2015). Design and Optimization of a 3-Coil Resonance-Based Wireless Power Transfer System for Biomedical Implants. *International Journal of Circuit Theory and Applications,* 43, pp. 1379–1390.

Yoon, I. J. and Ling, H. (2011). Investigation of Near-Field Wireless Power Transfer under Multiple Transmitters. *IEEE Antennas and Wireless Propagation Letters,* 10, pp. 662–665.

Zhang, F., Liu, J., Mao, Z. and Sun, M. (2012). Mid-Range Wireless Power Transfer and its Application to Body Sensor Networks. *Open Journal of Applied Sciences,* 2, pp. 35–46.

Zhang, H., Lu, F., Hofmann, H., Liu, W. and Mi, C. C. (2016). A Four-Plate Compact Capacitive Coupler Design and LCL-Compensated Topology for Capacitive Power Transfer in Electric Vehicle Charging Application. *IEEE Transactions on Power Electronics,* 31, pp. 8541–8551.

Zhang, J., Yuan, X., Wang, C. and He, Y. (2017). Comparative Analysis of Two-Coil and Three-Coil Structures for Wireless Power Transfer. *IEEE Transactions on Power Electronics,* 32, pp. 341–352.

Zhang, W., White, J. C., Abraham, A. M. and Mi, C. C. (2015a). Loosely Coupled Transformer Structure and Interoperability Study for EV Wireless Charging Systems. *IEEE Transactions on Power Electronics,* 30, pp. 6356–6367.

Zhang, W., Wong, S.-C., Tse, C. K. and Chen, Q. (2014a). Analysis and Comparison of Secondary Series and Parallel-Compensated Inductive Power Transfer Systems Operating for Optimal Efficiency and Load-Independent Voltage-Transfer Ratio. *IEEE Transactions on Power Electronics,* 29, pp. 2979–2990.

Zhang, Y., Lu, T., Zhao, Z., Chen, K., He, F. and Yuan, L. (2015b). Wireless Power Transfer to Multiple Loads Over Various Distances Using Relay Resonators. *IEEE Microwave and Wireless Components Letters,* 25, pp. 337–339.

Zhang, Y., Zhao, Z. and Lu, T. (2015c). Quantitative Analysis of System Efficiency and Output Power of Four-Coil Resonant Wireless Power Transfer. *IEEE Journal of Emerging and Selected Topics in Power Electronics,* 3, pp. 184–190.

Zhang, Z. and Chau, K. T. (2015). Homogeneous Wireless Power Transfer for Move-and-Charge. Overview of Wireless Power Transfer Technologies for Electric Vehicle Battery Charging. *IEEE Transaction on Power Electronics,* 30, pp. 6213–6220.

Zhang, Z., Chau, K. T., Liu, C., Qiu, C. and Lin, F. (2014b). An Efficient Wireless Power Transfer System with Security Considerations for Electric Vehicle Applications. *Journal of Applied Physics,* 115, p. 17A328.

Zhang, Z., Chau, K. T., Qiu, C. and Liu, C. (2015d). Energy Encryption for Wireless Power Transfer. *IEEE Transactions on Power Electronics,* 30, pp. 5237–5246.

Zhang, Z., Pang, H., Georgiadis, A. and Cecati, C. (2019). Wireless Power Transfer—An Overview. *IEEE Transactions on Industrial Electronics,* 66, pp. 1044–1058.

Zhong, W. and Hui, S. Y. R. (2015). Maximum Energy Efficiency Tracking for Wireless Power Transfer Systems. *IEEE Transactions on Power Electronics,* 30, pp. 4025–4034.

Zhong, W. and Hui, S. Y. R. (2018). Maximum Energy Efficiency Operation of Series-Series Resonant Wireless Power Transfer Systems Using On-Off Keying Modulation. *IEEE Transactions on Power Electronics,* 33, pp. 3595–3603.